ELECTROCHEMICAL REDUCTION OF AQUEOUS URANIUM

by

Jonathan M. Scaggs

A thesis

submitted in partial fulfillment

of the requirements for the degree of

Master of Science in Chemistry

Boise State University

December 2013

BOISE STATE UNIVERSITY GRADUATE COLLEGE

DEFENSE COMMITTEE AND FINAL READING APPROVALS

of the thesis submitted by

Jonathan M. Scaggs

Thesis Title: Electrochemical Reduction of Aqueous Uranium

Date of Final Oral Examination: 18 October 2013

The following individuals read and discussed the thesis submitted by student Jonathan M. Scaggs, and they evaluated his presentation and response to questions during the final oral examination. They found that the student passed the final oral examination.

Dale D. Russell, Ph.D.	Chair, Supervisory Committee
Brad P. Bammel, Ph.D.	Member, Supervisory Committee
Eric C. Brown, Ph.D.	Member, Supervisory Committee

The final reading approval of the thesis was granted by Dale D. Russell, Ph.D., Chair of the Supervisory Committee. The thesis was approved for the Graduate College by John R. Pelton, Ph.D., Dean of the Graduate College.

DEDICATION

I dedicate this thesis to my family and friends who have stuck through me through good times and bad. I am truly blessed to have their continued support. This is to my loving wife Carrie who has endured many long nights of research, writing, or other academic pursuits, which took my attention away from her. I will always appreciate her tolerance and unending patience for me and my academic pursuits.

ACKNOWLEDGEMENTS

I would like to express my gratitude to my graduate committee members for all of their effort, useful guidance, helpful remarks, and tireless guidance through the process of completing this thesis. Furthermore, I would like to thank Dr. Dale Russell for providing a never ending supply of patience, understanding, and wisdom that not only helped me academically but mentored me to become a research professional. I would also like to thank the staff and faculty of the Department of Chemistry at Boise State University for providing an excellent academic environment for the pursuit of this thesis.

ABSTRACT

The electrochemical reduction of uranium in acidic aqueous environments with the express purpose of generating U(III) consistently is critically evaluated. Generating U(III) in an aqueous environment is difficult and extremely unstable and has historically been difficult to achieve and isolate for further investigation. The electrochemical cell, electrodes, supporting electrolytes, and pH's are all reviewed and evaluated for the purpose of optimizing the systemic requirements to electrochemically generate U(III). Several new types of electrochemical cells to include two new spectroelectrochemical for UV-Vis and FT-Raman investigation were designed and tested for the purpose of analyzing the redox species of aqueous uranium generated while a reduction potential is applied to the cell. The new methodology developed demonstrated that U(III) could be generated electrochemically in the new cells and could be verified spectroscopically.

TABLE OF CONTENTS

LIST OF TABLES

LIST OF FIGURES

LIST OF ABBREVIATIONS

BDDE	Boron Doped Diamond Electrode
CE	Counter Electrode
CPE	Controlled Potential Electrolysis
CV	Cyclic Voltammetry or cyclic voltammetric scan
DOE	Department of Energy
EPA	Environmental Protection Agency
FPs	Fuel Pellets
FT-IR	Fourier Transform Infrared (spectrometer)
FT-Raman	Fourier Transform Raman (spectrometer)
IHM	Initially Present Heavy Metals
LSV	Linear Sweep Voltammetry
MA	Minor Actinides
MOX	Mixed Oxide (fuels)
MWD	MegaWatt-days
NRC	Nuclear Regulatory Commission
NWTRB	The Nuclear Waste Technical Review Board

RE	Reference Electrode
SE	Supporting Electrolyte (solution)
SEC	Spectroelectrochemical Cell
UHP	Ultra High Purity
UV-Vis	Ultraviolet-visible light (spectrometer)
WE	Working electrode

CHAPTER ONE: INTRODUCTION AND BACKGROUND

Presently in the United States, there is no universally accepted plan for the storage or reprocessing of national nuclear waste generated by energy producing facilities or from military nuclear asset destruction. The "legacy" waste we carry forward from all past nuclear enterprise activities has an ever increasing impact on the environment and thus on our society, and with no plan in place to rectify this situation, it portends a grim future of large scale radioactive waste storage areas. Historically, due to prolonged activities of nuclear energy production, military programs, and mining of uranium, the United States has accrued many sites that are currently radioactive and may remain so for hundreds to thousands of years. As of 2008, in the United States, the Department of Energy (DOE) states there are millions of gallons of radioactive waste as well as thousands of tons of spent nuclear fuel and material. In addition, there are huge quantities of contaminated soil and water, which threaten the safety of our future populations [1]. Despite large quantities of waste, the DOE has stated a goal of cleaning all presently contaminated sites successfully by 2025, although no specific plan to do so has been approved [1]. One example is the Fernald, Ohio, site, which had 31 million pounds of uranium product, 2.5 billion pounds of waste, 2.75 million cubic yards of contaminated soil and debris. A 223 acre portion of the underlying Great Miami Aquifer has uranium levels above drinking water standards.[1] To make this even more sobering, the United States has over 108 identified sites designated as areas that are contaminated and unusable due to radioactive contamination or storage. Many of these occupy

thousands of acres with the potential of growing larger until we can identify a real long-term solution.[1]

The DOE has been charged to clean or mitigate many or all 108 plus sites by the year 2025, even though this task may be difficult to impossible to achieve. They acknowledge that some may never be completely remediated. In just one of the previously mentioned 108 sites, at one of the larger areas located at the Oak Ridge National Laboratory, there were identified 167 individual and distinct, known contaminant release sites in one of the three subdivisions of the 37,000-acre area.[1]

There is still much in the way of radioactive, more importantly, radiotoxic material stored throughout the United States. There is definite need not only to reduce the amount of what is stored from past activities but also to find a way to reduce the amount of waste generated by ongoing, present energy producing activities. Current plans to deal with the accumulation of nuclear waste are: (i) continued storage on site in large cooling ponds; (ii) dry cask, above ground storage, (iii) deep bore hole storage, (iv) deep sea storage, (v) space storage, (vi) storage in a stable geological repository underground, (vii) transmutation, and finally, (viii) the recycling and reprocessing of nuclear material for further energy production.[4][5][6] Time is a major factor when considering storage because wherever this material is stored, it will remain hazardous for a very long time. The time estimated for reducing radioactive levels from ongoing nuclear enterprise back to planetary background levels ranges from 10,000 to 1,000,000 years according to half-life studies.[2] The long-term problem of current and future radioactive waste is a deep concern and has led to the emphasis on finding a permanent solution for this material as well as mitigating our health risk. Solutions such as the geological repository at Yucca

Mountain were until the past few years the short term answer for the storage of current waste. Plans for a geologic repository have been cancelled and another solution is now required.[3]

There has been a push internationally to reduce the overall accumulation of radiotoxic material resulting from nuclear energy while still meeting the national energy production requirements. Other options are being considered for long-term storage, remediation, or reuse. Dry cask storage is the most common above ground storage method used in the US. This involves storing waste originating from a spent fuel pool by first sealing it in a steel cylinder and then surrounding that with a concrete jacket, which acts as a radiation shield. This method is inexpensive and can be performed at the nuclear material generating facility. The waste can be easily retrieved for reprocessing if this becomes a viable option at some point.[5][6] Another option considered by several countries is preparing deep repositories for long-term storage of spent fuel and high level waste. This differs from the Yucca Mountain site in that while both involve a large stable geologic formation isolated from aquifer systems, the deep repository depends on a large-bore tunnel excavated miles into the earth's crust. At the bottom of this tunnel, rooms are created for the storage of radiotoxic materials.[4][5] The goal, like other plans, is to isolate the waste from the environment and from civilization. Even this method is temporary and the long-term ramification of the waste remains since many radioactive species have half-lives longer than one million years. Even with low container leakage, radionuclide migration rates must be taken into account.[7] It is estimated that it will take several hundred thousand years, perhaps upwards of several million years, to fully realize the benefits from waste isolation.[8] Another deep burial option is that of burial in the ocean.

Studies have been conducted over a 25-year period demonstrating that deep water takes 140 years to mix with shallow water in the North Atlantic based on analyzing oxygen content.[9] One plan is to bury nuclear waste beneath a stable abyssal plain in a subduction zone, which would slowly carry the waste downward into the earth's mantle. This procedure allows for the earth to bury the waste naturally before any potential radioactive waste leaks could circulate in the environment. While this seems like a strong proposal, it requires international cooperation, and would require a rewrite of the international "law of the sea."[10][11] Even so, the subduction zone burial method has been described as the most viable means of disposing of radioactive waste, and is still considered one of the premier disposal methods.[12][13]

Another active avenue of research is transmutation of radioactive waste into less harmful waste products while also deriving energy from the process. One reactor, the Integral Fast Reactor, was a proposed nuclear reactor with a nuclear fuel cycle that produced no transuranic waste and was designed to consume the byproducts of nuclear power generation. It proceeded as far as large-scale tests, but was then canceled by the US Government due to fears of plutonium proliferation.[14] While this technology was cancelled in the US, other countries in Europe continued to pursue the idea and as a result there are several reactors capable of transmutation while producing energy. The United States is now also actively conducting research on transmutation technologies that would significantly reduce the need for nuclear waste treatment and storage.[15] There are several reactors currently in European Union (EU) that transmute a volume equivalent to the entire annual minor actinide production from the reactors presently operating in the

United States fleet, while simultaneously generating approximately 1 gigawatt of power from each reactor annually.[16]

Many of the options proposed are simply short-term plans; the need for a long term solution to the problem still exists. With the long-term geological repository Yucca Mountain no longer an option and other smaller sites throughout the US reaching their storage capacities in the near future, it is imperative to find another way either to reuse the spent nuclear fuel or to make it far less hazardous. Current US planning is to establish, as of 2010, the Blue Ribbon Commission on America's Nuclear Future.[17] This Commission, composed of fifteen members, conducted an extensive two-year study of nuclear waste disposal of the nuclear energy process.[17] The Commission established three subcommittees: Reactor and Fuel Cycle Technology, Transportation and Storage, and Disposal, and in January 2012, the Commission submitted its final report.[17] During their research, the Commission visited current leaders in the research of nuclear energy and nuclear waste handling and storage: Finland, France, Japan, Russia, Sweden, and the UK.[18] As a result, in the final report, the Commission put forth seven recommendations for developing a comprehensive strategy to pursue.[18] These recommendations are the following: (1), the United States should undertake an integrated nuclear waste management program that leads to the timely development of one or more permanent deep geological facilities for the safe disposal of spent fuel and high-level nuclear waste. (2), A new, single-purpose organization is needed to develop and implement a focused, integrated program for the transportation, storage, and disposal of nuclear waste in the United States. (3), Assured access to the balance in the Nuclear Waste Fund (NWF) and to the revenues generated by annual nuclear waste fee payments from utility ratepayers is

absolutely essential and must be provided to the new nuclear waste management organization. (4), A new approach is needed to site and develop nuclear waste facilities in the United States in the future. It is believed that these processes are most likely to succeed if they are (as quoted directly from the Blue Ribbon Commission report to President Obama in December 2012):

> (i) Adaptive—in the sense that process itself is flexible and produces decisions that are responsive to new information and new technical, social, or political developments.[18]
>
> (ii) Staged—in the sense that key decisions are revisited and modified as necessary along the way rather than being pre-determined in advance.[18]
>
> (iii) Consent-based—in the sense that affected communities have an opportunity to decide whether to accept facility siting decisions and retain significant local control.[18]
>
> (iv) Transparent—in the sense that all stakeholders have an opportunity to understand key decisions and engage in the process in a meaningful way.[18]
>
> (v) Standards- and science-based—in the sense that the public can have confidence that all facilities meet rigorous, objective, and consistently-applied standards of safety and environmental protection. Governed by partnership arrangements or legally-enforceable agreements with host states, tribes and local communities.[18]

(5), The current division of regulatory responsibilities for long-term repository performance between the NRC and the EPA is appropriate and should continue. The two agencies should develop new, site-independent safety standards in a formally coordinated

joint process that actively engages and solicits input from all the relevant constituencies.[18] (6), The roles, responsibilities, and authorities of local, state, and tribal governments (with respect to facility siting and other aspects of nuclear waste disposal) must be an element of the negotiation between the federal government and the other affected units of government in establishing a disposal facility. In addition to legally-binding agreements, as discussed in Recommendation #4, all affected levels of government (local, state, tribal, etc.) must have, at a minimum, a meaningful consultative role in all other important decisions. Additionally, states and tribes should retain—or where appropriate, be delegated—direct authority over aspects of regulation, permitting, and operations where oversight below the federal level can be exercised effectively and in a way that is helpful in protecting the interests and gaining the confidence of affected communities and citizens.[18] Lastly, (7), The Nuclear Waste Technical Review Board (NWTRB) should be retained as a valuable source of independent technical advice and review.[18]

This national plan has led to heavy research emphasis across the US to find a permanent solution to the mounting nuclear waste situation, all the while maintaining a high level of nuclear energy production, and simultaneously decreasing the probability of contributing to the proliferation of weapons grade nuclear materials. The concept of a closed nuclear fuel cycle is not new but it is problematic. As nuclear fission occurs, a stream of radioactive and non-radioactive material is produced. The waste stream is a mixture of most of the elements found on the periodic table (Figure 1.1). Of highest interest is the mixture of lanthanides and actinides.

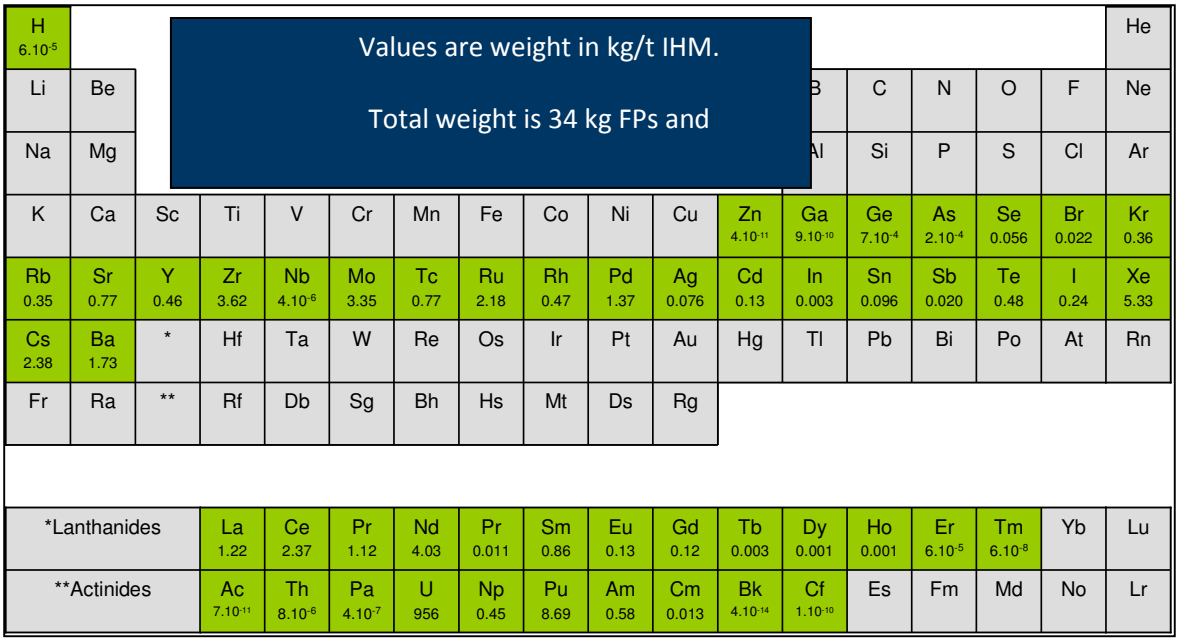

Figure 1.1 Values are weight in kg/t IHM (Initially present Heavy Metals). Total weight is 34 kg FPs (fuel pellets) and 9.7 kg transuranic elements, 956 kg UO_2 remains. Calculated composition after 10 yr cool of 1 ton U as 3.2% enriched UO_2 fuel with 33 MWd/kg (Megawatt-days) U burn-up at a mean flux of 3.28×10^{18} n m^{-2} s^{-1} in a typical PWR, courtesy of INL.

There are well developed processes for extracting uranium and plutonium, e.g. UREX or PUREX, from the waste stream for further use. The remaining radioactivity occurs primarily because of the presence of the minor actinides, especially neptunium, americium, and curium. Their removal by any known technology is complicated by the presence of the lanthanides.

The goal in a closed nuclear reactor is to recycle as much as possible back into energy production. Any element that cannot be recycled must be transmuted into a stable isotope. For instance, uranium and plutonium can be reprocessed into mixed oxide (MOX) fuels and transmuted in standard reactors. The heavier elements could be transmuted in fast reactors.[19] Isotopes of actinides tend to be long-lived with half-lives of many thousands of years, whereas radioactive fission products tend to be shorter-lived

(most with half-lives of 30 years or less). From a waste management viewpoint, transmutation of actinides eliminates a very long-term radioactive hazard and replaces it with a much shorter-term one.[19]

If transmutation occurs to the transuranic elements such as the isotopes of plutonium, neptunium, americium, and curium, it has the potential to help solve the problems posed by the management of radioactive waste, by reducing the proportion of long-lived isotopes contained and potentially creates more energy in the process. When irradiated with fast neutrons in a nuclear reactor, these isotopes can be made to undergo nuclear fission, destroying the original actinide isotope and producing a spectrum of radioactive and nonradioactive fission products.[19]

See Figure 1.2 through Figure 1.4 to illustrate the difference between a "once through" nuclear cycle with a single reprocess/recycle step with possible U enrichment

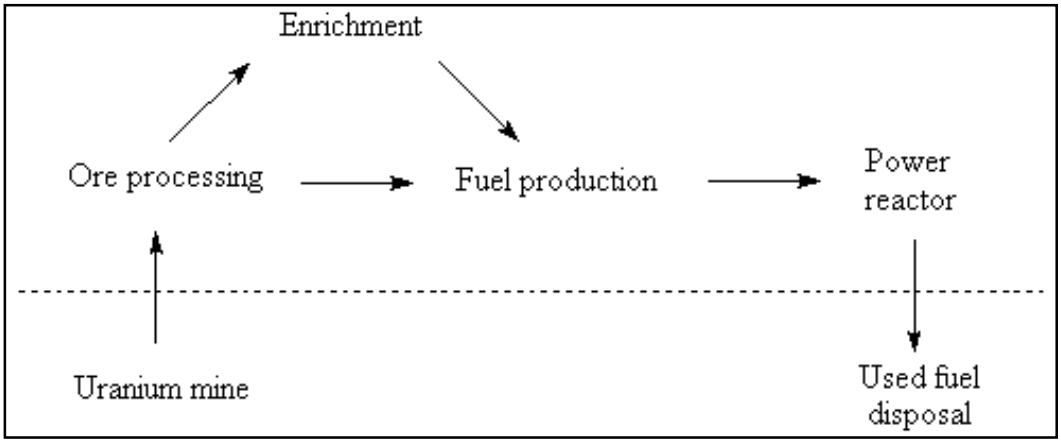

Figure 1.2 A once through generic (or open) fuel cycle

(Figure 1.2), to a recycle schematic showing an integral fast reactor recycling minor actinides for energy production as well as reprocessing U and Pu for further use (Figure 1.4). In a single pass through a nuclear reactor, fuel is used once and then sent to storage

without further processing except for additional packaging, which some consider better for the environment and society.

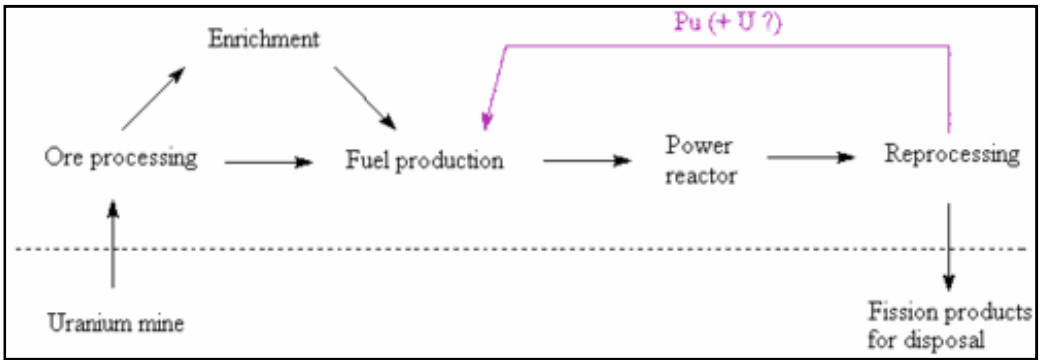

Figure 1.3 A fuel cycle in which plutonium is used for fuel

This method is used extensively by the United States, Canada, Sweden, Finland, Spain, and South Africa.[20] In the US, this stored waste is not considered available for future energy production, however, countries such as Sweden and Canada have designed repositories to permit future recovery of the material should the need arise.[20][22]

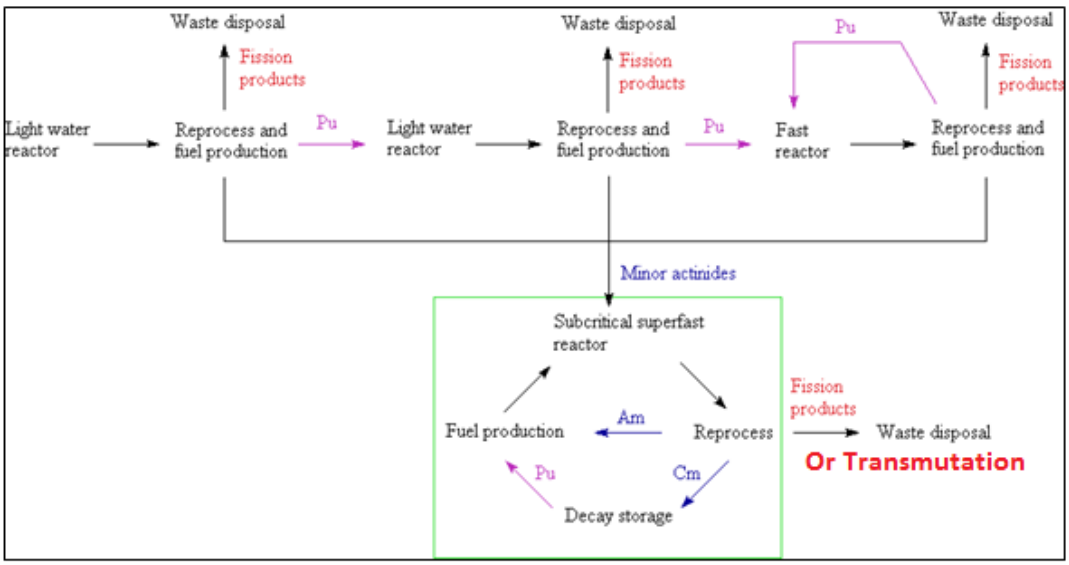

Figure 1.4 A pair of fuel cycles in which uranium and plutonium are kept separate from the minor actinides. The minor actinide cycle is kept within the green box.

In contrast, several countries including Japan, Switzerland, and previously Spain and Germany, are using or have used the reprocessing services offered by British Nuclear Fuels Limited (BNFL) and AREVA. The BNFL is a nuclear energy and fuels company owned by the UK Government. It was a former manufacturer and transporter of nuclear fuel, MOX, and managed reactors. They generated and sold electrical power as well as reprocessing and managing spent fuel throughout the EU. The AREVA (formerly Cogema) La Hague site is an AREVA nuclear fuel reprocessing plant in La Hague on the French Cotentin Peninsula that currently has nearly half of the world's light water reactor spent nuclear fuel reprocessing capacity where it extracts plutonium and produces MOX fuels.[27] Here, the fission products, minor actinides, activation products, and reprocessed uranium are separated from the reactor-grade plutonium, which can then be fabricated into MOX fuel.[19][20] Because the proportion of the non-fissile even-mass isotopes of plutonium rises with each pass through the cycle, there are currently no plans to reuse plutonium from used MOX fuel for a third pass in a thermal reactor shown in Figure 1.3. However, if fast reactors become available, they may be able to burn these, or almost any other actinide isotopes.[19][20] It is a major goal to develop a process where actinides other than uranium and plutonium, such as the minor actinides, are used in critical power production in addition to reprocessing spent primary fuel, while reducing an additional nuclear waste from continued power production.[21]

A problem arises due to the difficulty in separating the minor actinides from the nuclear waste stream after U and Pu have both been removed. Developing a method for

separating these two groups is of great interest to the nuclear community and is the fundamental focus of this project. The 14 elements that comprise the lanthanide series are formed when uranium and plutonium undergo nuclear reactions and are thus present in nuclear waste stream as seen in Figure 1.1. The 4f sub-level contains seven orbitals, each of which will hold two electrons, allowing for a total of 14 electrons. Generally speaking, the lanthanides have electron configurations that follow the Aufbau rule. The 4f sublevel is filled as atomic number increases from cerium to lutetium. However, there are three lanthanide metals that have properties similar to the d block: Ce, Lu, and Gd. These three metals contain only one d electron in their ground state configuration. A similar overall trend holds for the 14 elements in the actinide series from thorium to lawrencium, where the 5f sublevel is progressively filled. The chemistry of the lanthanides differs from main group elements and transition metals because of the nature of the 4f orbitals (Figure 1.5)**.** These orbitals are "buried" inside the atom and are shielded from the atom's environment by the 4d and 5p electrons.

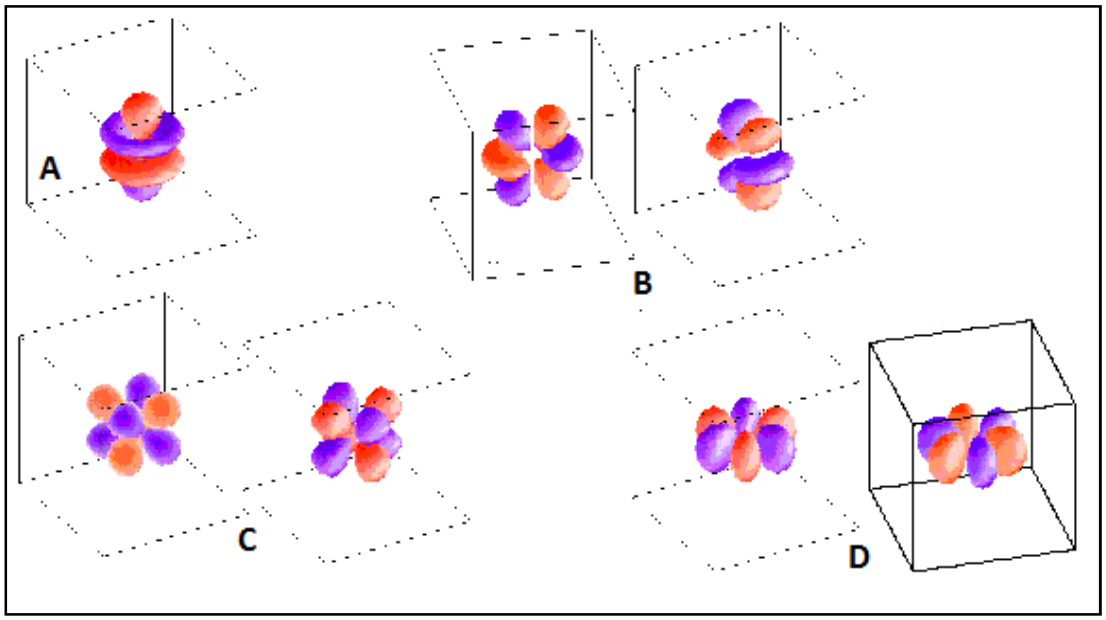

Figure 1.5 This figure illustrates the f orbitals (l-3). A – $f_z^3 = f_z(2z^2-3x^2-3y^2)$ $[m_l=0]$; B – $f_{xz}^2 = f_x(4z^2-x^2-y^2) + f_y(4z^2-x^2-y^2)$ $[m_l=\pm1]$; C – $f_{xyz} + f_z(x^2-y^2)$ $[M_l=\pm2]$; D – $f_x(x^2-3y^2) + f_y(3x^2-y^2)$ $[m_l\pm3]$

As a consequence, the chemistry of the elements is largely determined by their size and charge, and thus is largely a function of surface charge density. Atomic size decreases gradually with increasing atomic number in a phenomenon known as the lanthanide contraction. All the lanthanide elements exist in nature and in solution as oxidation state +3. Aberrations from this rule are Ce^{+3}, which can lose an f electron to form Ce^{+4} gaining the stability of the Xe electron configuration. Another is Eu^{3+}, which can gain an electron to become Eu^{+2} giving it the stability of a half-filled f^7 configuration.[22][23][24][25]

Actinides are typical metals in that they are soft, malleable, metallic, and lustrous. They readily oxidize in air. Unlike the lanthanides, most elements of the actinide series have the same properties as the d block elements. Members of the actinide series can lose multiple electrons to form many different ions. All actinides are radioactive, paramagnetic, and, with the exception of actinium, have several crystalline phases. All actinides are pyrophoric, especially when finely powdered or given sufficient surface area in contact with air. The lanthanides are highly reactive with halogens and chalcogens, and the actinides are even more reactive with these species. Actinides, especially those with a small number of 5f electrons, are prone to hybridization. This is explained by the similarity of the electron energies at the 5f, 7s, and 6d shells. Most actinides exhibit a larger variety of valence states, and the most stable are (+6) for uranium, (+5) for protactinium and neptunium, (+4) for thorium and plutonium, and (+3) for actinium and other actinides.[22][23][24][25]

The reduction potentials as determined by thermodynamic calculation and by several electrochemical methods are shown in Table 1.[28][29] Only a few are included in this table, as they are involved in the previously mention UREX and PUREX processes.

Table 1.1 Standard reduction potentials of select actinides in an acidic solution (V vs SHE).[23][24][25]

Actinide (M)	MO_2^{2+}	MO_2^{+}	M^{4+}	M^{3+}
U	0.07	0.62	-0.63	-1.66
Np	1.13	0.7	0.15	-1.8
Pu	0.94	1.04	0.98	-2.0

These values derive from ideal aqueous conditions and it is important to note these reduction values are dependent on many experimental parameters such as supporting electrolyte (SE), pH, dissolved gasses, electrodes, and temperature. For species with higher oxidation states such as U(VI), the oxycation, uranyl (UO_2^{2+}) forms readily and is the most stable and therefore the most prevalent aqueous uranium species.

The similarities in size and charge are what lead to the principal difficulty in separating the two categories of elements. The minor actinides could be separated or transmutated easily if were not for the presence of the lanthanides with them in the waste stream. Neutron bombardment of the minor actinides is made inefficient due to the lanthanide absorption of the neutrons and their separation is extremely difficult due to nearly identical size, surface charge density, and chemical behavior and reactivity.[22]

A selective ligand has been identified that binds to the minor actinides in the presence of the lanthanides and can be used to transport the actinides across a phase boundary in a solvent extraction process. This ligand is a polyfluoridated dithiophosphinic acid, which was designed by a team of collaborators at the Idaho National Lab.[61][62] The hypothesis is that the minor actinides favor coordination with a

more covalent coordination sphere and softer donor atoms. In contrast, the lanthanides have different frontier orbital types and favor more ionic coordination. This is a very subtle difference. Optimizing the extraction efficiency requires either a great many extraction steps or, more efficiently, even more selective ligands. A fundamental goal for this project is to elucidate the mechanism of coordination, and either prove or disprove this hypothesis. If proven, it is at least theoretically possible to design more selective ligands.

The proof of the hypothesis depends on eliminating all experimental variables except the covalency vs. ionicity of the coordination sphere, which in turn requires all ions to be in the same oxidation state. Therefore, the reduction of thorium, uranium, and plutonium is undertaken, in order to match the +3 oxidation state of the minor actinides and all of the lanthanides.[30]

Uranium was examined in this work because the natural abundance isotope is relatively inexpensive and relatively safe to work with. It does not require extraordinary security and containment measures, as would for example, americium or plutonium. Reduction of the uranyl ion was performed via systematic electrochemical protocol. This process remains a clean chemistry and is a simpler, more efficient process, which produces less waste than would a chemical reduction process.[30][31][32][33][34][39]

Uranyl, UO_2^{2+}, is a stable, abundant, naturally occurring U(VI) species, which is used predominantly in this study. Starting with this oxidation state, the systematic reduction is undertaken to achieve the other oxidations states, U(V), U(IV), and U(III) . It is important to note that both U(V) and U(III) are extremely reactive and unstable. U(III) is a powerful reducing agent and reduces water to hydrogen gas. All reductions were

conducted via electrochemical methods. The practice of electrochemical reduction and subsequent extraction is consistent with uranium extraction processes presently in place in reactor facilities and would therefore be easily adapted to current technology. In addition, electrochemical reduction is a clean, continuously reusable process, producing very little in the way of additional waste products.[26][39] In this work, uranium was reduced electrochemically until U(III) was achieved in direct electron transfer method from an inert cathode, to create an actinide analogue to compare with the other actinides and with similar lanthanides (all 3+ oxidation state). Further study is planned to measure and characterize the covalency of the resulting coordination sphere, when the dithiophosphinic acid is introduced. The ultimate goal is to design an efficient method to extract the minor actinides from aqueous mixtures containing the lanthanides. Once removed, the minor actinides would be either recycled into power production or transmuted via neutron bombardment.

Such a separation method will be one giant step towards creating a closed nuclear fuel cycle.

CHAPTER TWO: MATERIALS AND METHODS

Materials

Reagents used to make supporting electrolyte (SE) solutions were ACS reagent grade and were used without further purification. These salts include KNO_3, $NaNO_3$, $NaClO_4$, (all from Fisher Scientific), and Na_3PO_4 (Sigma Aldrich). The only exceptions are KCl and NaCl (both from Fisher Scientific), which were further purified by double recrystallization from ethanol. All acids used were ACS reagent grade with the exception of HNO_3 which was "nanopure" metals grade and was only used as a supporting electrolyte. This HNO_3 was used without further purification. The metals grade HNO_3 was stored separately from all other reagents and kept in a nitrogen cabinet.

The $UO_2(NO_3)_2 \bullet 2H_2O$ and $UO_2HPO_3 \bullet 2H_2O$ reagents were purchased from Alfa Aesar and were ACS reagent grade and used without further modifications. The pitchblende containing U(IV), was from “New Brunswick Laboratories, Atomic Energy Commission” and was reagent grade. The pitchblende was processed through an acid digestion before use.

The platinum foil electrodes were 99.99% pure from Alfa Aesar. The electrodes were polished with alumina paste and then sonicated and washed in a nitric acid wash. When in use, the electrodes were thoroughly cleaned before every electrochemical scan in nitric acid and then flamed to incandescence. The platinum wire was also purchased from Alfa Aesar and was 99.98% pure. The platinum wire when used as a counter

electrode was rinsed in concentrated nitric acid, rinsed in DI water and then flamed to incandescence between uses.

Another electrode used extensively was boron doped diamond (BDD), which was purchased through Element 6. A 1 cm^2 square electrode was used in many standard electrochemical experiments as was a 1 cm (diam) round electrode for rotating disk experiments. Both BDD electrodes were electrochemically conditioned in a 0.5 M HNO_3/0.5 M $NaNO_3$ solution prior to use. This is discussed in greater detail later in this chapter. The BDD electrodes were thoroughly cleaned between uses with a nitric acid wash.

Water used to make supporting electrolyte solutions and analytical solutions was distilled to 18MΩ standards with a Barnstead Nanopure™ Infinity water purifier system.

All gases used in experiments were purchased from Norco, Inc in Boise, ID. Nitrogen was either pre-pure (PP) quality for many of the standard electrochemical experiments but in some cases was ultra-high purity (UHP). In both cases, the N_2 gas was channeled through a $CaCl_2$(s) gas filter before entering the electrochemical cell. The argon used in the glove box experiments was UHP and was purchased from Norco, Inc of Boise, ID.

Methods

All electrochemical experiments were conducted with either an EG&G PAR 263A potentiostat/galvanostat or a EG&G PAR 273 potentiostat/galvanostat under a nitrogen atmosphere.

Three different electrochemical methods were employed throughout this work. They are controlled potential electrolysis, linear sweep voltammetry, and cyclic voltammetry. Controlled Potential Electrolysis (CPE) was employed when only the oxidized species was initially present. In that case, the potential is set at a constant value sufficiently negative to cause rapid reduction of the analyte species desired and is maintained at this value until only the reduced species is present in solution. The total charge (Q) passed during the CPE experiment is calculated by integrating the current with respect to time, and is related to the number of electrons transferred per molecule (n) and the number of moles of the oxidized species initially present (N) through Faraday's law:

$$Q = nFN \qquad (1)$$

F is Faraday's constant (96485 C mol^{-1}). If either n or N is known, the other can be calculated from the integrated current, assuming no other solution species is electroactive at the same potential.[31][32][33][34][38]

Voltammetry, either as linear sweep voltammetry (LSV) or cyclic voltammetry (CV), is the predominant technique employed in this work. Voltammetry applies a constant and/or varying potential at an electrode's surface and measures the resulting current. This work used a three electrode system. This method can reveal the reduction potential of an analyte and its electrochemical reactivity. This method in practical terms is nondestructive because only a very small amount of the analyte is consumed, transformed, or adsorbed at the surface of the working or counter electrode, which can in theory be recycled if the reverse process can be made to occur, for example, by reversing

a scan, or stepping to a potential that reverses the electrochemical process of the first step. In the voltammetry experiment, the electrical potential waveform is applied to the working electrode. This waveform may be a triangle wave, sine wave, square wave, or even a sawtooth waveform. The potentiostat is able to initiate the waveform at any part of the cycle, and to set the potential range, sweep rate, and switching potentials of the waveform.[31][32][33][34][40]

In the rotating disk electrode experiment, an electrical potential waveform is applied to a disc shaped electrode that is rotated in the solution, thus causing convection to occur in a mathematically predictable way. The diffusion layer thickness of the solution at the surface of the rotating electrode can be calculated from the rotation speed and the kinematic viscosity of the fluid. The rotating disk working electrode replaces the fixed, static working electrode in a three electrode system. The disk's rotation is usually described in terms of angular velocity (ω). As the disk turns, some of the solution described as the hydrodynamic boundary layer is dragged by the spinning disk and the resulting centrifugal force flings the solution away from the center of the electrode. Solution flows up, perpendicular to the electrode, from the bulk to replace the boundary layer. The sum result is a laminar flow of solution towards and across the electrode. The rate of the solution flow across the electrode can be controlled by the electrode's angular velocity and modeled or predicted mathematically. This flow can quickly achieve conditions in which the steady-state current is controlled by convection rather than diffusion. This is a contrast to quiescent solutions used in cyclic voltammetry where the steady-state current is limited by the diffusion of the electroactive species. By running linear sweep voltammetry in conjunction with the rotation disk electrode experiments at

various rotation rates, different electrochemical phenomena can be investigated, including single or multi-electron transfer, the kinetics of a slow electron transfer, adsorption/desorption steps, and electrochemical reaction mechanisms that include heterogeneous and homogeneous steps (EC, ECE, etc.).[31][32][33][34][40]

The Electrochemical Cell Considerations

Generic bulk electrochemistry was conducted in a small 25 mL glass cell, which was "electrochemical method clean"*[1]. In general, all cells will have a similar functional design even though they will differ when it comes to specific purpose. The bulk cell had two conductive electrodes, the anode and the cathode. The anode is defined as the electrode where oxidation occurs and the cathode is the electrode where the reduction takes place. In between these electrodes is the supporting electrolyte, which contains mobile charge carriers, the ions, which can freely move and facilitate current flow. The supporting electrolyte also serves to suppress the migration of the analyte in the electrical field so that its bulk transfer kinetics are determine by diffusion and convection, only. In all cases, the counter electrode was a platinum flag. The working electrode was either a platinum flag or a boron doped diamond electrode (BDDE). In addition, a third electrode is used to serve as the reference electrode. In all experiments, the reference electrode was a BASi RE6™ Ag/AgCl (Sat KCl) electrode. See Figure 2.1 below. Nitrogen is used to purge all dissolved gases from the solutions. During the electrochemical process, nitrogen was also flowed over the solution surface to prevent any atmospheric gases from reentering the solution during experiments.

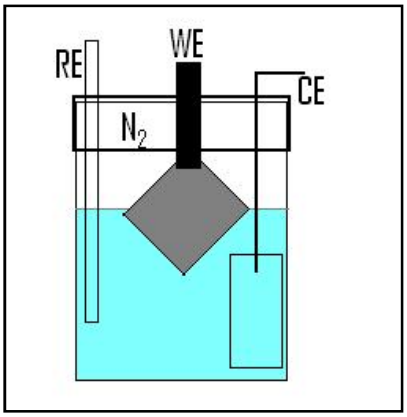

Figure 2.1 A simple bulk cell design with a traditional hanging electrode design. This figure shows a square BDD working electrode suspended partially in the electrolyte solution.

The predominantly used electrochemical cell was a low volume, corrosion cell (BioLogic A-011951), which had a total volume of 0.95 mL and was made of poly tetrafluoroethylene (PTFE). The cell will be referred to as the minicell and can be seen in Figures 2.2 and 2.3. In the minicell, the working electrode is either Pt or BDDE. When the BDDE is the working electrode it is necessary to use a Pt contact pad between the potentiostat lead and the electrode. Figure 2.2 shows a gold foil pad in place of the platinum. Also a coiled Pt wire is used instead of a flag due to space limitations. When the cell is completed, the working electrode is sandwiched between the upper and lower PTFE blocks with a nitrile O-ring placed in direct contact to prevent leaks. Nitrogen is used to purge other dissolved gasses in the solutions and then flowed over the top to prevent any atmospheric gases from re-entering the solutions. In Figure 2.2 there are two ports on either side of the CE pin, which facilitate the flow in and out of nitrogen through the cell.

Figure 2.2 This figure shows the minicell fully assembled and ready for use in the far left panel. The connection pin is shown for the counter electrode as well as the RE6 reference electrode protruding from the top of the cell. The center panel shows the individual components in an exploded view. The far right panel shows the BDDE on my hand for perspective. Either a Pt or BDD working electrode was used in the minicell.

The PTFE mini cell allows for a very controlled solution volume and "head space", which does a couple of things. The first is this design allows for a great degree of control of the system allowing for fewer possible sources of contamination, either chemical or physical. The other is that this design permits for the generation of a small amount of waste.

Standard electrochemical experiments have been conducted in a small, 10mL single compartment, or 30 mL 3 compartment glass cell, Pt working electrode (WE), Pt counter electrode (CE), and a Ag/AgCl (Sat KCl) reference electrode. The mini cell (see Figures 2.2 – 2.5, and Figure 3.0) has a smaller volume of 0.90 mL, uses a boron doped diamond electrode (BDDE) working electrode, a Pt CE, and a BASI® Ag/AgCl(Sat KCl) reference electrode. All solution was purged with ultra-high purity (UHP) N_2 for 10 minutes prior to and electrochemical experiments and the same N_2 gas was continuously flowed over the top of the solution during experiments to prevent the re-adsorption of

atmospheric gases into the solution. The BDDE was a square ($1cm^2$ x 1mm) electrode, which was clipped by one corner with an alligator clip and then dipped into the SE as consistently as possible (see Figure 2.1) so that 1 cm^2, front and back, was exposed to the analyte for each experiment. The PTFE minicell was used for most of the remaining experiments for many reasons. This arrangement is superior in many ways to the traditional electrochemical cell and a necessity for the reduction scheme of uranium.

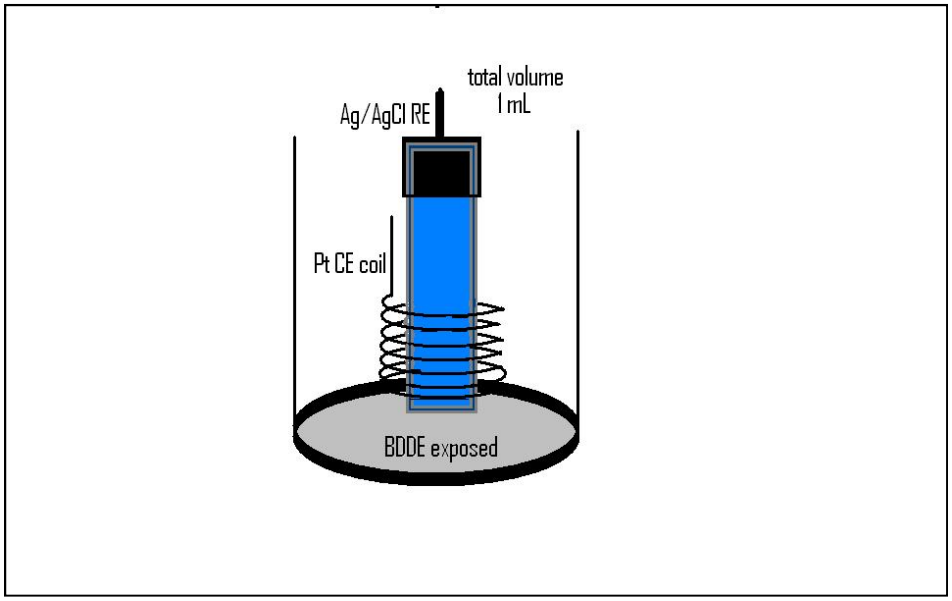

Figure 2.3 The internal arrangement of the minicell. The WE forms the bottom of the cell, the reference electrode is inserted into the supporting electrolyte and the counter electrode is wound around the reference electrode without touching either of the other electrodes.

The minicell, as seen in Figure 2.3, had a working volume of less than 1 mL, making it ideal for the analysis of uranium by not creating much in the way of actinide waste but still allowing for complete and thorough analysis. Also, the minicell system allowed for the easy control of the atmosphere since the headspace was very small and easy to maintain a N_2 environment over the test solutions. The minicell, a glass cell, a

BDDE, and the Pt working electrode all have their place and are all useful. In this case, a minicell was used predominately due to the ability to control the experimental environment. As the for the time and place for the different working electrode's, a series of residual curves are demonstrate the effect on the supporting electrolyte solution by changing the different working electrode (BDDE for Pt), the SE's (KNO_3, KCl, $KClO_4$, $NaNO_3$, and NaCl), and the pH (1, 2, 3, 4). These conditions were tested for several reasons. One, it is important to identify any potential interference that may arise from systemic conditions before the uranium is introduced into the study. Any experimental condition found that may give an interference or problem was no longer used. Two, to identify the optimal set of conditions that would give the best result and allow for the greatest level of control in the experiments. Three, hopefully this process will help create a process to remove MA's from a complex waste stream by using uranium as an analogue.

The third cell type used is a jacketed rotating disk electrode experimental cell (see Figure 2.4). This cell is very similar to the bulk electrochemical cell except that the cell has a well at the bottom where the shaft of the working electrode sits. The working electrode is a flat circular surface that is oriented horizontally and is parallel to the bottom of the cell. The working electrode was either a Pt disk electrode or a custom made BDDE disk electrode. The Pt disk electrode was purchased from PINE™ was purchased at the same time as the shaft and rotator assembly. The WE, whether BDD or Pt, is encased in a PTFE sleeve, which excludes solution even at high rotational speeds. The CE was Pt and the reference electrode was the BASi RE6™. The rotating disk

electrochemical cell was purged with N_2. This cell has a special feature, namely a jacket, which allows for the operator to control the temperature of the experiment.

Figure 2.4 A typical jacketed rotating disk electrode cell. This image (courtesy of BASi) is a small volume three electrode cell with gas purge holes in the PTFE lid. The total volume for this cell is 25 mL with a 10 mL well.

There advantages and disadvantages to each of the materials used for the working electrodes in this work. Several factors were considered in making the choice of which to use. The platinum electrode is a noble metal film and is easier to clean of adsorbed surface contaminants because it can be heated to incandescence in an oxidizing flame prior to use. The platinum is stable to short-term heating, and is relatively inert both chemically and electrochemically. It is difficult to oxidize and it is unreactive in most environments, including concentrated strong mineral acids. The preparation requirements for the Pt working electrode are simple. It is polished with alumina, rinsed in DI water, washed in concentrated HNO_3, and rinsed in DI water again. The disadvantage of the Pt electrode is that is has a narrow accessible potential range and is catalytic for the reduction of H+ to H_2 gas on the surface before 1.0 V in the reduction

scheme. The working range of the Pt working electrode is roughly -0.5 to 1.0 V dependent on pH, temperature, and the presence of chemical modifiers. In contrast, the BDDE has a much larger dynamic working range from -2.5 to +3.0 V.[35][36][37][41] This material is also robust and unreactive to even strong concentrated mineral acids and extremely strong reducing agents. The negative aspect of the BDDE is that it has a rough surface, which allows materials to build or adsorb and also allows for small leaks in the minicell. The BDDE required preconditioning with 0.5 M $NaNO_3$/0.5 M HNO_3 solution, held at +3.0 V for 30 minutes. The BDDE must be cleaned and preconditioned on a regular basis, which requires several hours taking away from analysis of the analytes. See Figure 5, which shows the smooth and rough surfaces of a typical BDDE.

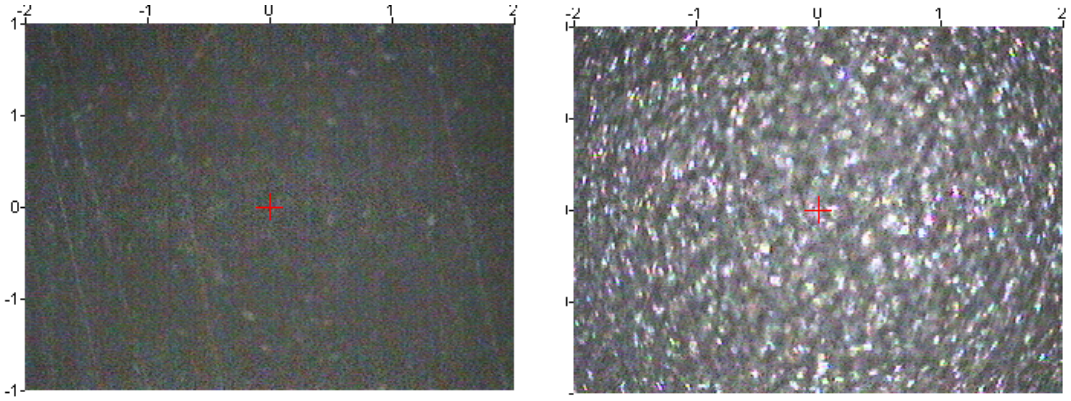

Figure 2.5 The smooth (left) and rough (right) surfaces on the 30x optical microscope.

Each BDDE has two very different surfaces. One side is smooth with a Ra of 30nm whereas the other is much rougher with a Ra of 100μm (average roughness factor, Ra, data provided by Sigma-6®) and consistent with values reported in literature.[35][36][37][41] The two sides provide drastically different landscapes, which have dramatic impact on surface area, electrochemical double layer, and interface with the supporting electrolyte

surface. These factors are uncontrollable, inconsistent, and highly variable from surface to surface. Another factor observed with the BDDE dipped into the supporting electrolyte is that solution creeps up the rough side of the electrode and comes in contact with the alligator clip. This does have a significant impact on the electrochemistry being measured as it adds electron transfer measurements not related to the analyte in solution.

Another important aspect of this work is optimizing the solution conditions that most facilitated the reduction of uranium. It was essential to determine which electrolytes and solutions worked the best. The solvents and electrolytes are described above. pH was maintained by titrating solution with acids containing the same anion and with bases with the same cation. The only exception to this is with perchlorates as no perchloric acid was used in this work. All stock analyte solutions were made using specific supporting electrolyte solutions weighing out analyte on a 4 place balance and diluting with high precision pipetors. All acids used in this work were ACS grade except for the occasional use of metals grade nitric acid.

Spectroscopic and Spectroelectrochemical Methods

A Cary 100 UV-Vis spectrometer and Thermo Nicolet FTIR/Raman were used to analyze solutions, analytes, and substrates. Many of the solutions and substrates could be analyzed with traditional techniques but to analyze the U(III) species specialized techniques and spectroelectrochemical cells (SEC) needed to be developed. See Figure 2.6 for the FT-Raman SEC, which was used in a 90^{o} reflecting Raman platform, allowing the incident light from the instrument to impact at 90^{o} to the BDDE face.

The specialized cell seen in Figure 2.6 was made from high density PTFE and was composed of three pieces. The face was predominately the cell volume and the

single quartz crystal window. The middle piece of the assembly contained the BDD working electrode and the large Pt counter electrode, which wrapped around the working electrode. When the face and middle part are placed together, there is only 1mm between the quartz window and the BDDE face. The last block of the body has channels for all electrodes to be connected to the potentiostat. The BDDE working electrode (WE) was preconditioned as described above, before each series of experiments in the SEC, the Pt electrode was flamed, and the reference electrode was rinsed and soaked in 1 M KCl. The PTFE body was washed in HNO_3 and then rinsed between every cycle. Parafilm was used as a gasket material between layers, and for each new experiment cycle a new gasket was used.

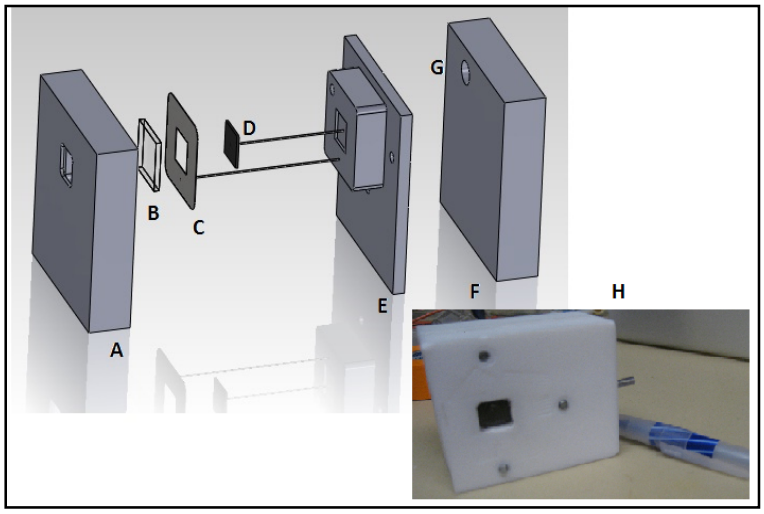

Figure 2.6 The FT-Raman SEC. The top right is a blow–up version where A is the face block, B is the single crystal quartz face, C is the platinum counter electrode, D is the BDDE working electrode, E is the PTFE block aligning all the electrodes and wires, and F is the support block to which the screws fasten. G shows where the BASi RE6 reference electrode inserts into the assembly. H shows the size of the SEC next to a pen for scale.

The UV-Vis SEC was used extensively in order to confirm the different oxidation states of the uranium in solution during controlled potential electrolysis. Figure 2.7 shows the

UV-Vis SEC in a schematic as well as in use outside the UV-Vis and in the Cary 100 UV-Vis. The SEC was composed of a standard UV-Vis quartz one-way cell. The custom made PTFE top served as a holder for all three electrodes but also as an airtight lid to prevent air from entering the system. The cell was thoroughly purged with N2 prior to sealing the top and conducting an experiment. Again, parafilm was used a sealing gasket and was discarded after every set.

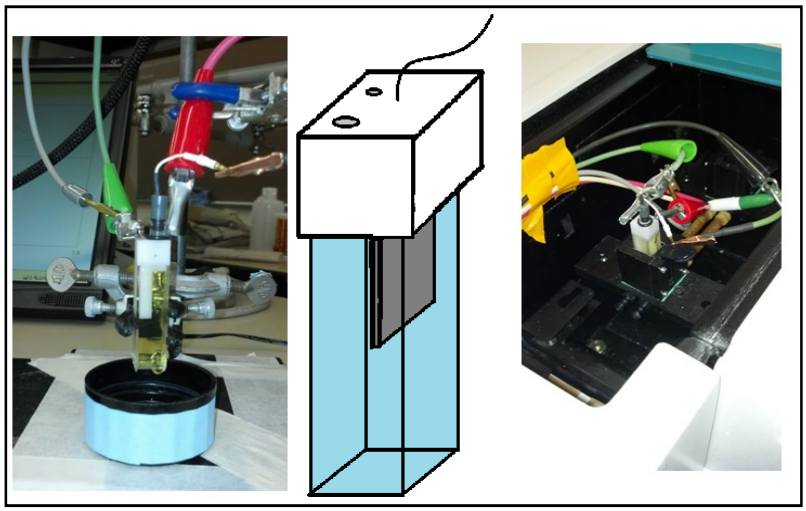

Figure 2.7 The UV-Vis SEC. This is a more simple assembly than the Raman SEC where the BDDE working electrode is aligned parallel to the incident light in the UV-Vis chamber. A shows the UV-Vis SEC with all electrode connections in a uranyl solution. B shows a basic schematic of the assembly where a single PTFE block houses all the electrodes and acts as a lid to the quartz cell. C shows the SEC in a Cary 100 UV-Vis spectrophotometer.

The SEC's made it possible to conduct CPE, LSV, and CV experiments while simultaneously analyzing spectroscopic data in real time. While it was possible to conduct each experiment (electrochemistry or spectroscopy) separately, it was important to combine the two to corroborate the oxidation states resulting from electrochemical inputs. The spectroelectrochemical experiments made this possible.

*[1] – “Electrochemical method clean” as described on page 21 refers to a process by which glassware is cleaned so that all inorganic and organic material has been removed from the glassware and will not introduce an interference. "Trace metals" concentrated nitric acid is used to wash the glassware, followed by a rinse with 18MΩ DI water, then alcoholic KOH is used to wash the glassware, followed by another 18MΩ DI water rinse. The glassware is then rinsed once more with the concentrated nitric acid followed by a final wash with 18MΩ DI water.

CHAPTER THREE: RESULTS

Optimization of Electrodes and Supporting Electrolytes

It was essential to find optimal working conditions conducive to the electrochemical reduction of uranium from the stable U(VI) to the very unstable and reactive U(III) in aqueous solution specific to a nuclear waste stream because this had not been previously reported in the literature. Most studies have either dealt with the complexation and chemical dynamic of U(VI) or used chemical reduction schemes with redox mediators and complex solutions.[30][42 - 51]There have been studies that measure uranium reduction in acidic and basic solutions. However, these were not in an effort to produce recoverable U(III) species. Therefore, a study of residual current curves was undertaken to examine the effects of various supporting electrolyte salts, dissolved gas effects, pH, and various electrode surfaces. Platinum and boron doped diamond electrodes (BDDE) were examined in various supporting electrolytes with and without nitrogen purge. The BDD electrode was used in several experiments due to the much larger voltage range relative to platinum. The discharge limit for the reduction of hydrogen was more than a volt greater than of platinum with the BDDE. For this reason, the BDDE was useful in exploring the reduction of uranium in multiple solutions when Pt was untenable. These differences are demonstrated in Figures 3.1 through 3.4.

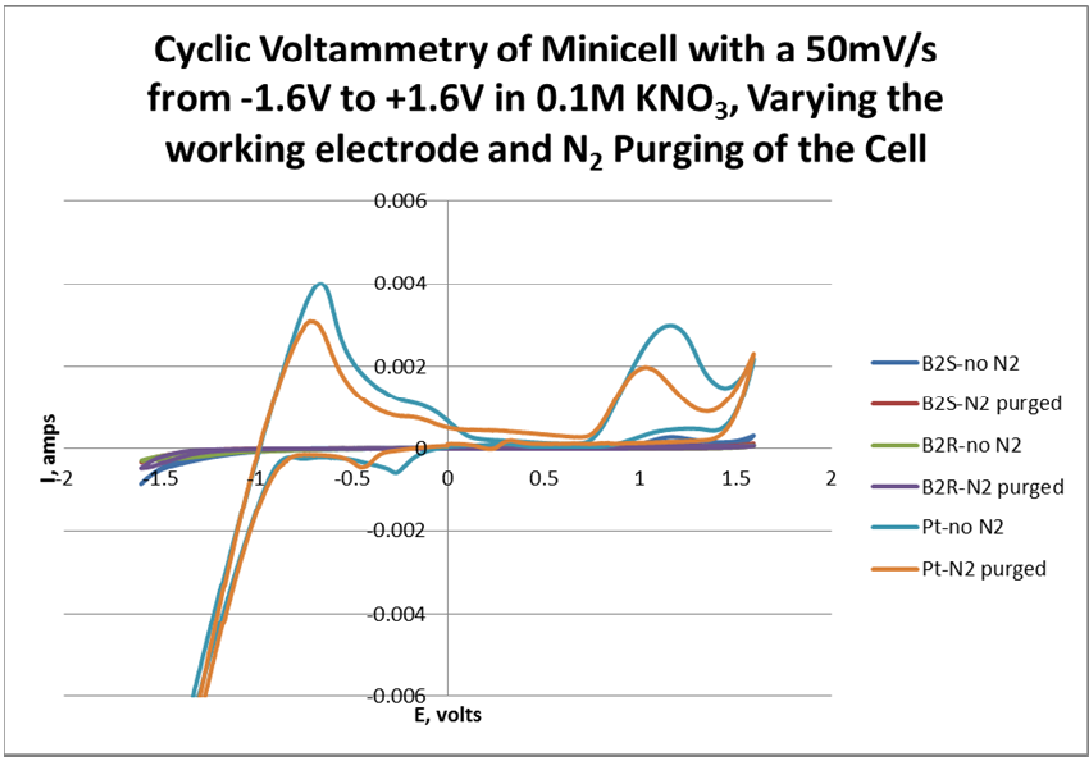

Figure 3.1 Comparison of BDD and Pt electrodes in KNO_3 solution with and without nitrogen purge showing differences in the residual current curves. The B2S and B2R represent two types of surfaces on a BDDE where "S" is smooth and "R" is rough.

Figure 3.1 shows that the discharge limit for Pt begins at about -1.0 volts for the reduction of hydrogen, as expected. The BDDE, which is directly compared to the Pt electrode in Figure 3.1 and then shown separately in 3.2, demonstrates a small residual current in the same range. Platinum also shows re-oxidation of hydrogen at -0.7 volts and also a solution based oxidation at approximately +1.3 volts. Purging with nitrogen reduces or removes electro-active species, presumably oxygen.

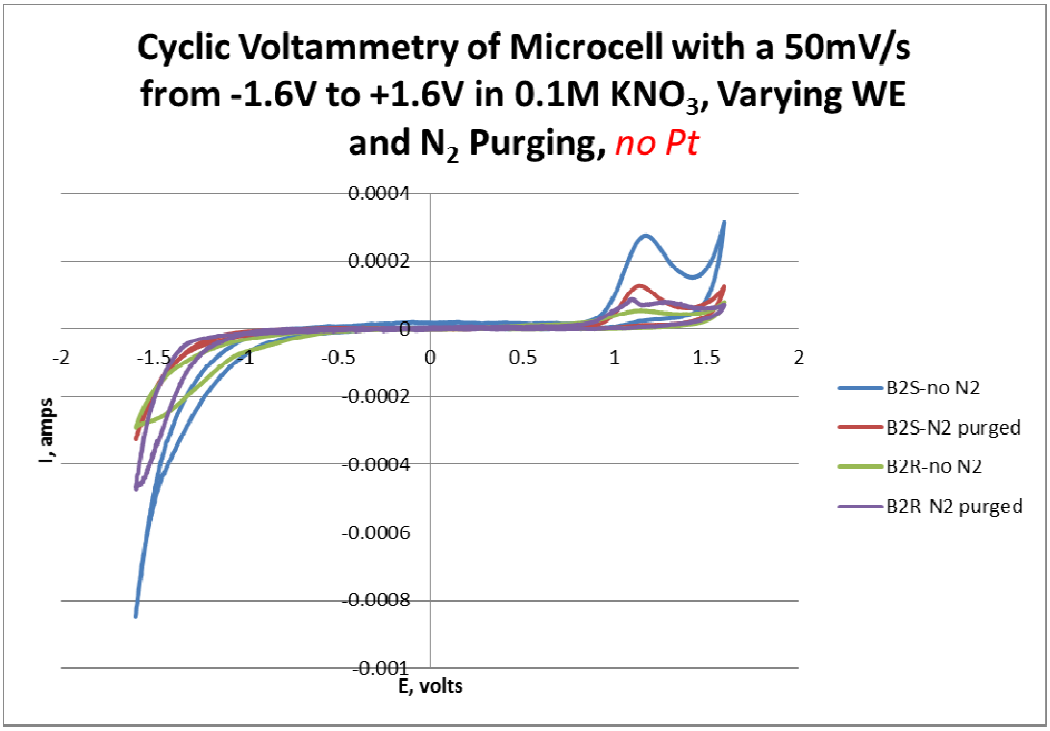

Figure 3.2 Comparison of the smooth and rough sides of the BDD electrode with and without nitrogen purge. Note the change in the Y-axis scale relative to Figure 3.1.

The CV overlay shown in Figure 3.2 demonstrates that the BDDE has a different residual current profile depending on surface roughness. BDD electrodes are grown with two sides, one side is polished smooth represented with the notation BS, and the other side is unpolished and rough, denoted by BR. The BDDE had a much higher over potential for the reduction of hydrogen than the platinum resulting in smaller residual current and a broad accessible cathodic range. As expected, higher surface roughness gives greater current response to both noise and signal due to increase in actual surface area. As before, purging with nitrogen removes oxygen from the solution, reducing those anodic features. Apparently the smooth surface supports oxidation of oxygen and also reduction of hydrogen better than the rough surface. It is important to note that the re-oxidation of hydrogen gas at -0.7 volts on the return scan is not observed.

With the BDDE, the residual current remained low until about -3.0 volts, making this range useable for cathodic studies,[5][6][7] which was only one of two primary working electrodes examined in this study. The rough side of the BDDE could not be made solution tight in the minicell setup. Cells in the configuration leaked and were not used in any further experiments.

All of the supporting electrolytes shown in this work will support the reduction of uranium with little to no solution based interference, however the $NaNO_3$ as seen in both Figures 3.3 and 3.4 show a greater intensity in the oxidative range, which could hinder anodic evaluation. Multiple electron transfer events most likely due to the oxidation of dissolved oxygen reduce the useable range making this electrolyte unfavorable for this project. This behavior was observed for both BDD and Pt electrodes. When $NaNO_3$ is used as the supporting electrolyte, the BDDE exhibits a much higher over potential for the reduction of hydrogen than the platinum resulting in smaller residual current and a broader, useable cathodic range. As expected, higher surface roughness gives greater current response to both noise and signal due to increase in actual surface area. As before, purging with nitrogen removes oxygen from solution, reducing the oxidative features in the anodic range.

As shown in Figure 3.3, the BDDE has smaller residual currents throughout the range shown. The Pt is catalytic for the reduction of hydrogen as seen in the large cathodic current starting at about -1 volt shown in Figure 3.4. Platinum also supports the oxidation of dissolved gases at about +1 volt, however these gases are removed by purging the solutions with nitrogen. The comparison of the useable range with KNO_3,

seen in Figure 3.3, is slightly larger than for $NaNO_3$ possibly due to the more cathodic potential for the reduction of the potassium ion versus that of the sodium ion.

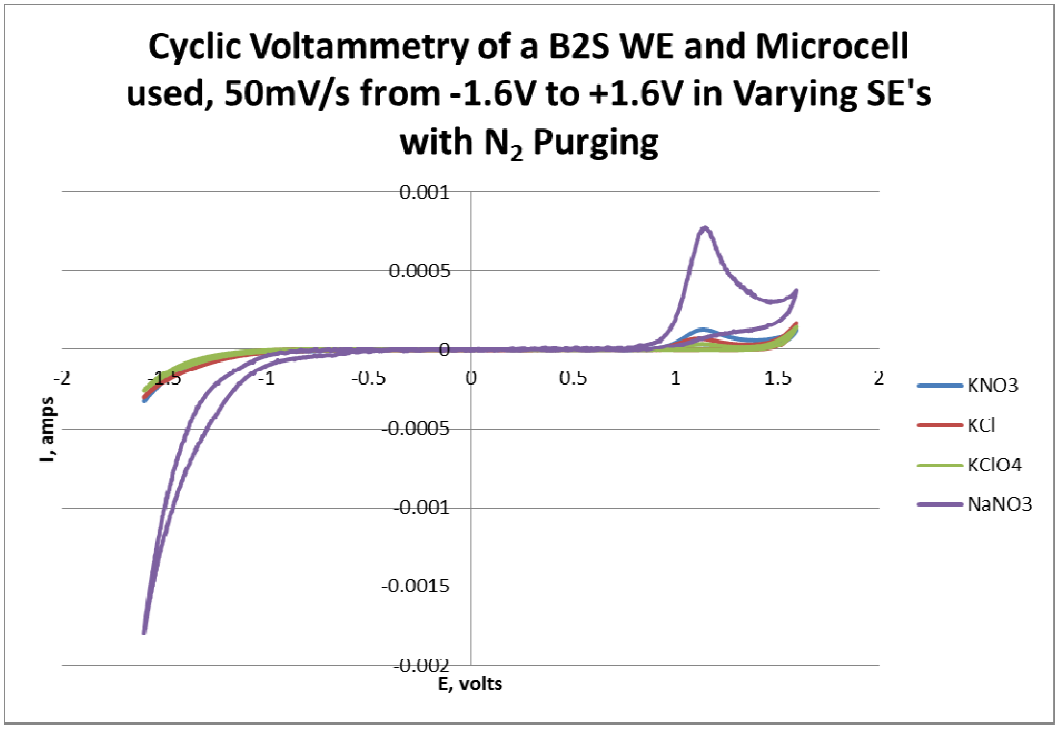

Figure 3.3 Overlay of residual current curve for four electrolyte salts on smooth side of a BDDE from +1.6 V to -1.6V. Note how flat and featureless the baselines are with only oxidation occurring at between +1.0 to +1.5 in these CV's.

There are six different supporting electrolyte compounds tested in this study where five are shown in Figures 3.3 and 3.4. The purpose of the multiple electrolytes is twofold. The first purpose is to determine if there is an optimal supporting electrolyte for the electrochemical reduction of uranium to U(III) with the smallest amount of solution based reductions. It is possible for solution-based redox events to interfere or obscure electron transfer events of uranium, which is why this step must be taken. The second purpose was to demonstrate that uranium could be reduced to U(III) consistently in several different electrolytes and on different electrodes in the minicell. The sixth

electrolyte, HNO_3, is discussed separately below in the experiments involving pH. There are no solution-based reductions occurring that will interfere with uranium reduction analysis between the discharge limits with either the BDD or Pt electrodes.

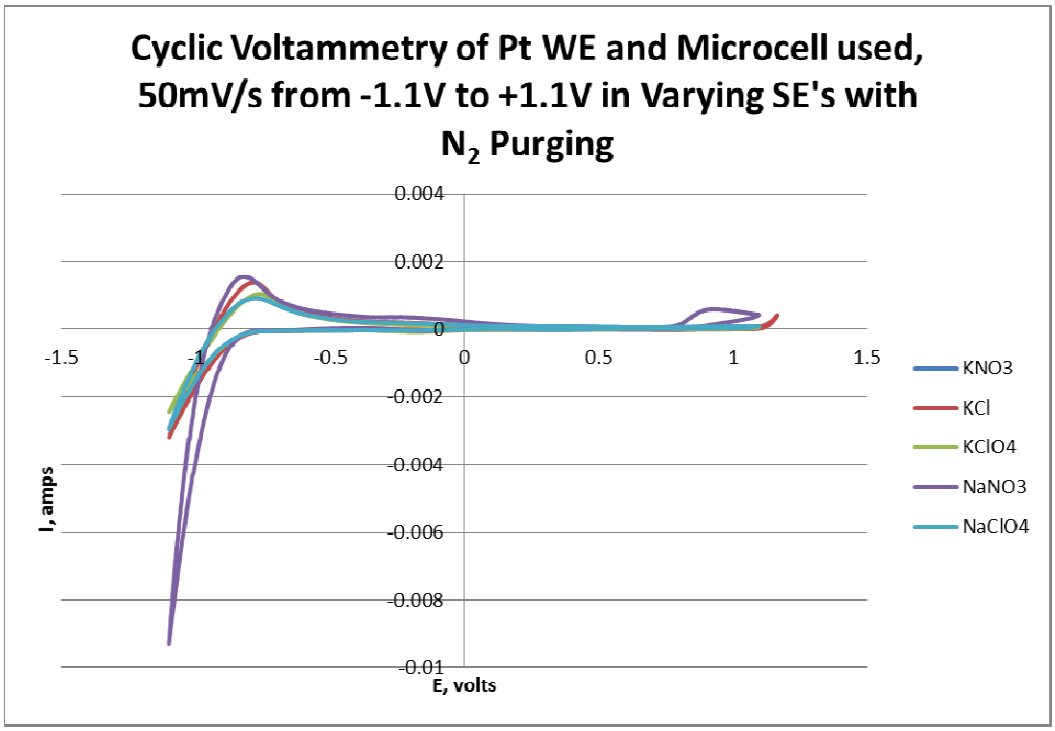

Figure 3.4 Overlay of residual current curve for five electrolyte salts on a Pt electrode from +1.1 V to -1.1 V. Reduction of hydrogen is occurring at about -1 volt.

The platinum electrode reduction of hydrogen is a consistent and prominent feature. However there is still a useable window between -0.9 volts and +0.8 V. Based on these experiments, KNO_3 was selected for further studies. In order to more closely resemble the waste stream from nuclear power generation pH studies were undertaken using either nitric or hydrochloric acids for pH adjustments. The nuclear waste streams are typically acidic with pH less than 2.

Both pH and common ion effects were considered. The uranium salt used in this study was uranyl nitrate ($UO_2(NO_3)_2 \cdot 2H_2O$) with the standard supporting electrolyte (SE hereafter) as 0.1 M KNO_3, pH adjusted using HNO_3or HCl. Several combinations of SE's and acids were analyzed to identify if there would be any complications due to an increase in the nitrate anion or a decrease in pH. The combinations are as follows for this study only: SE1 is KNO_3/HNO_3; SE2 is KNO_3/HCl; SE3 is KCl/HNO_3; and SE4 is KCl/HCl.

Reduction potential is a function of pH as can be seen in Figure 3.5. As pH decreases, the reduction potentials shift to higher potentials overall and become closer together, requiring less energy for each electron transfer. The figure shows the redox potential as a function of pH with the key representing uranium oxidation state changes. For this reason and also to emulate the conditions expected in a nuclear waste stream, the reduction of uranium was examined at low pH solution conditions.

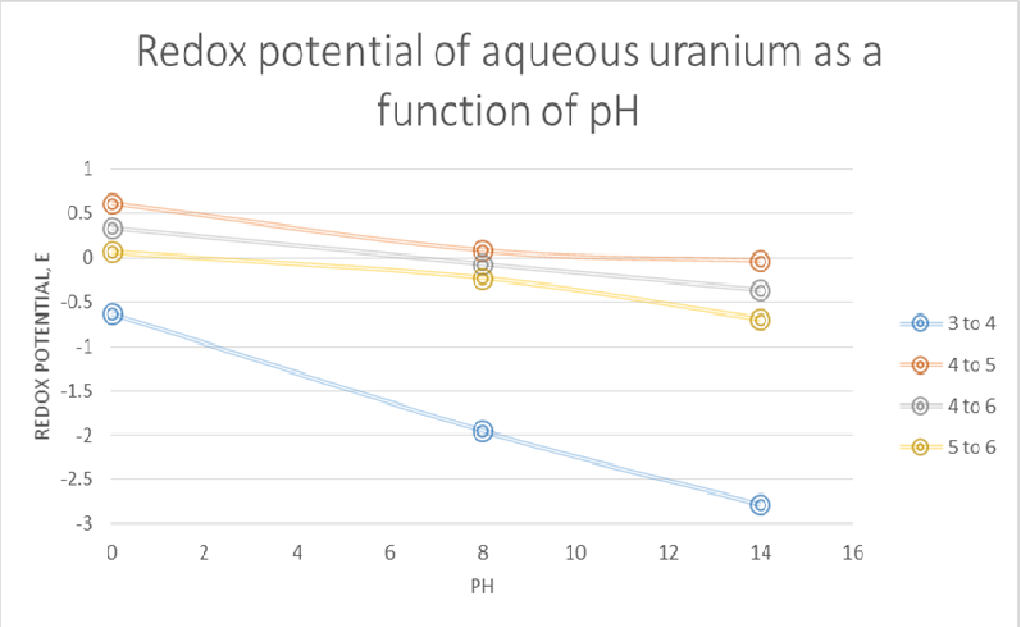

Figure 3.5. The effect of pH on the reduction potentials of uranium. As the pH decreases, the reduction occurs at lower potential and the potential difference between steps is reduced.[24][25]

The next few figures show the details of the effect of pH on the minicell makeup and the solution. As shown in Figures 3.6 and 3.7, each combination of SE and acid was examined via cyclic voltammetry (CV), and the resulting voltammograms overlaid for comparison. There are no prominent electron transfer events in the negative voltage ranges arising from the common ion, however the lower pH increases the current arising from reduction of H^+, as expected. The optimal pH for this study was determined to be pH 2.0, which is consistent with in the composition of nuclear waste streams. This corresponds well with the reduction of uranium shown in Figure 3.5, where the reduction steps from U(VI) to U(V) to U(IV) to U(III) are all much closer together.

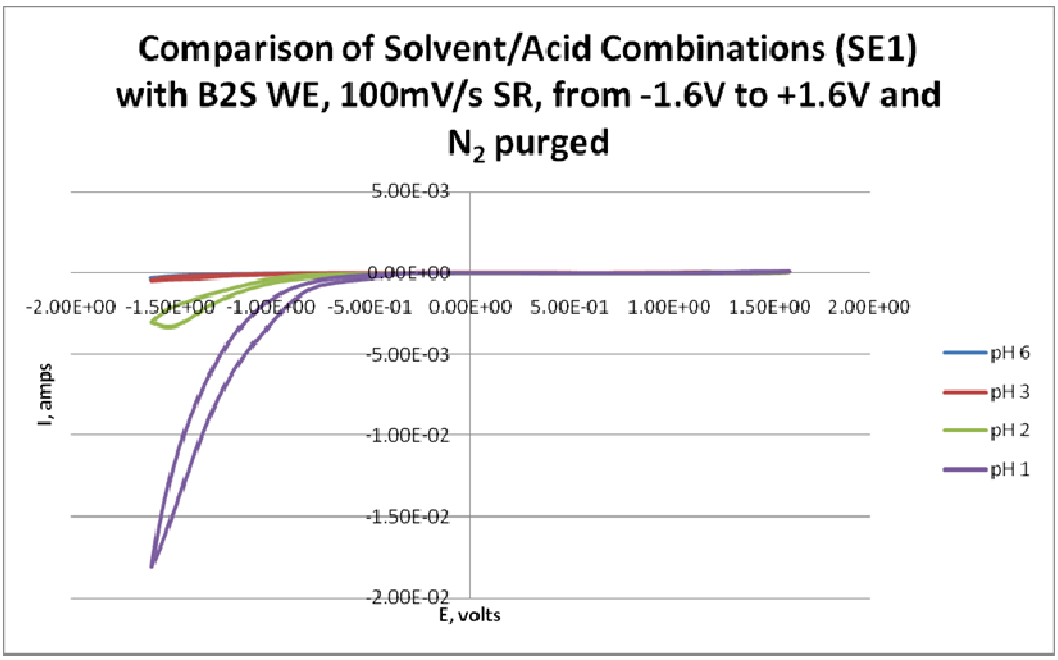

Figure 3.6 Comparison of residual current curves for KNO_3 at different pH's as adjusted by HNO_3. Other than the evidence of more H+ production at the cathode, there is no negative impact of low pH on the electrochemical system. Note the scale on the current axis.

Figure 3.6 SE1, which is KNO_3/HNO_3, shows 4 overlaid CV's at different pH's, which demonstrate an increase in the baseline current due to increased hydrogen reduction. The pH 1 residual curve has the largest baseline current with a peak current of -1.78×10^{-2} A at -1.6V due to the increased level of free H^+ in solution. All of the supporting electrolyte /acid combinations behaved in a similar fashion, as can be seen in Figure 3.7. In this figure only, the pH 2 CV's are shown since this is the target pH of further analysis with the uranium reduction. This pH is also within the range as would be seen in a reactor waste stream. And even though the KNO_3/HNO_3 had the largest residual curve baseline, we still continued to use this combination as it is the predominant electrolyte and acid within the waste stream.

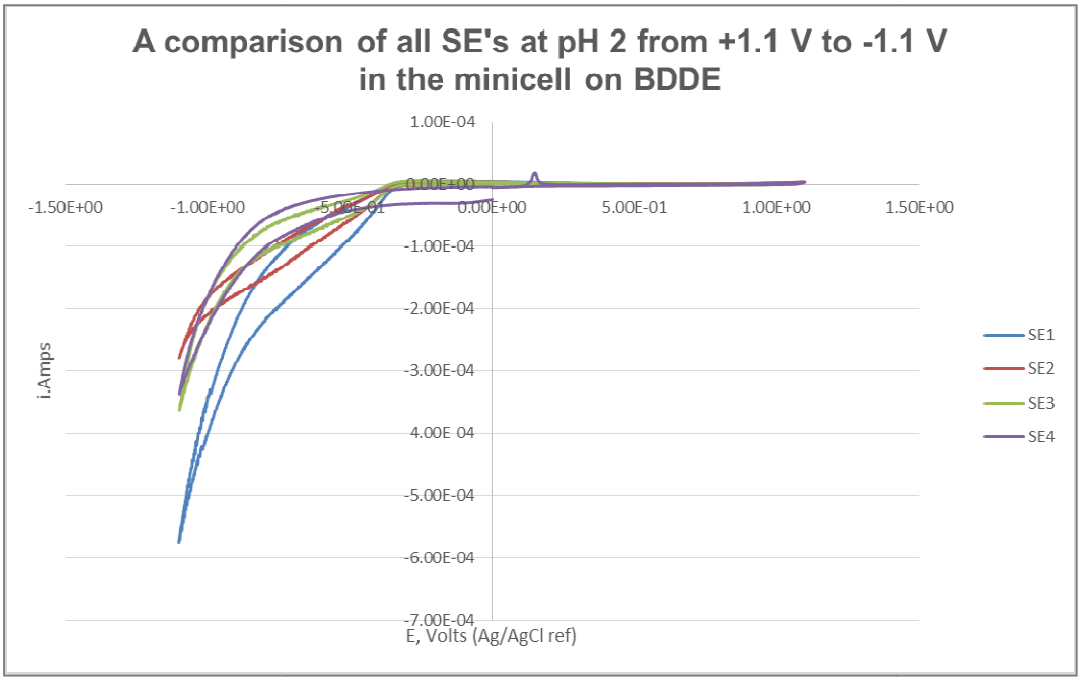

Figure 3.7 Comparison of all for SE's and acids at pH2. For this specific study SE1 is KNO_3/HNO_3, SE2 is KNO_3/HCl, SE3 is KCl/HNO_3, and SE4 is KCl/HCl

These findings suggested the following conditions for the reduction of uranium. The minicell is used due to its small volume, which generates smaller volumes of hazardous waste. Also, the smaller cell was easier to insulate against temperature fluctuations and mechanical vibration, both of which cause noise in the electrochemical data. The rough side of the BDD electrode was no longer used because of cell leaking. Therefore, either platinum or the smooth side of the BDDE was used. The BDDE gives a broader, useful potential range, but the Pt is much more sensitive as indicate by greater currents for all observed processes. Hydrogen reduction occurs but is easily identified. The operational pH for the rest of the studies with uranium was at pH 2.0, adjusted with HNO_3, verified via Thermo Orion pH meter at frequent intervals.

Uranium Reduction Results

The results from this study may one day be used to find a way to separate minor actinides from a nuclear waste stream containing lanthanides and other fission products. Therefore, conditions used for the reduction of uranium were made as similar as possible to the waste stream, specifically ionic strength is high and pH is low. Figure 3.8 shows a 25 mM uranyl nitrate solution overlaid with two residual curves. One curve is a 0.1M KNO_3 solution at pH 6 and the other at pH 2.

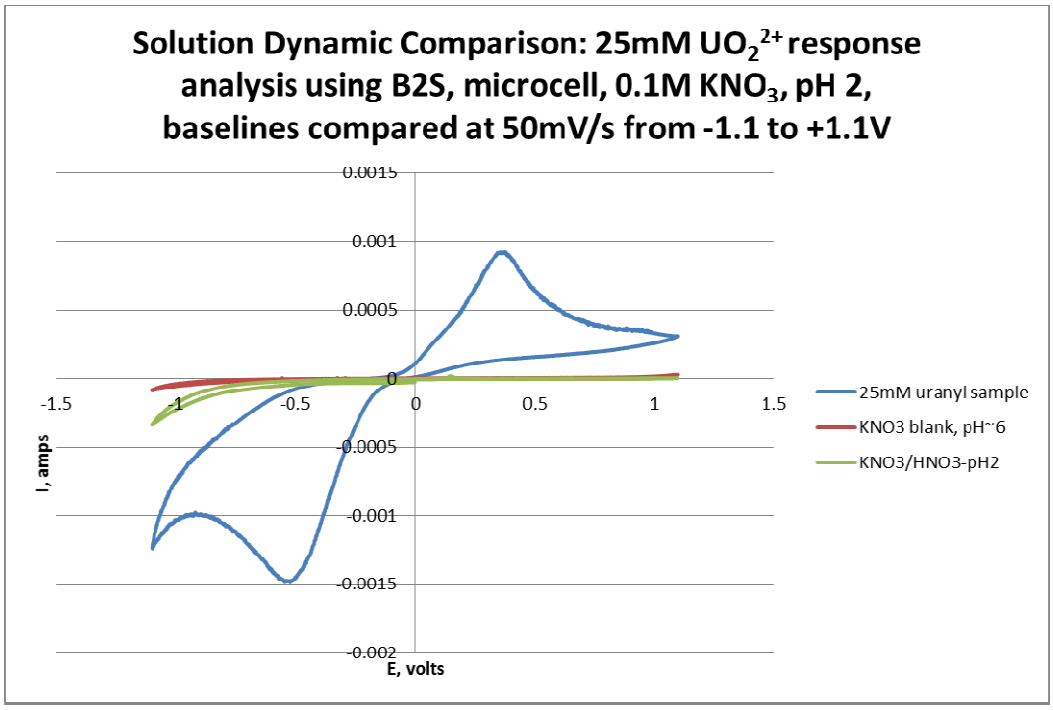

Figure 3.8 Overlay of three CV's on BDDE. The red CV is of a 0.1 M KNO_3 SE at pH 6. The green CV is of a 0.1 M KNO_3 SE at pH 2.0, and the blue CV is a 25 mM solution of uranyl nitrate. All CV's are between +1.1 and -1.1 V cycled at 50mV/s

There is a scale difference between the three curves and it is obvious there is no contributing interference from the residual curves. This is consistent throughout this study and the baseline CV's will not be shown in further CV overlays.

A N_2 gas purged 12.5 mM uranyl nitrate 0.1 M KNO_3 solution was placed in the minicell with a BDDE working electrode, a Pt wire counter electrode, a BASi Ag/AgCl (sat KCl) reference electrode, and analyzed in several voltage ranges and scan rates.

Initial work placed a large emphasis on the BDDE as the working electrode in the electrochemical cell due to the hypothesis that hydrogen reduction would interfere with uranium reduction in the cyclic voltammogram. The BDDE had many advantages, such as being robust, chemically and physically inert, and it had a very large dynamic range, allowing for "large" voltages to be used, at least in the electrochemical sense of the word. After preconditioning, the BDDE was an excellent choice for electrochemical work with the only two drawbacks being the price of making a reproducible surface, and that because it is a semiconductor, it is not as sensitive as Pt. A series of experiments was conducted to determine the voltage needed for each reduction step for uranium; +6 to +5, +5 to +4, and +4 to +3. It was also if interest to determine if there were homogeneous steps in the overall mechanism, and lastly to see if the kinetics of each step could be determined.

As shown in Figure 3.8 above, a single large reduction peak is observed (there is also a single large oxidation peak). From this data, it was impossible to know if all three steps were occurring in a concerted mechanism or if one or more steps required more cathodic potential to occur. Therefore, a scan rate dependence study was conducted with both working electrodes and supporting electrolytes as shown in the next several figures. Half of the studies conducted were on BDD and the other half were on Pt working electrodes. The next series of figures show both. Figures 3.9 through 3.13 are all conducted on BDDEs, whereas Figures 3.14 through 3.16 are all conducted on Pt

working electrodes. Both electrode types are shown to represent that the reductions occur on both but in different locations, as would be expected between a conductor (Pt) and a semiconductor (BDDE).

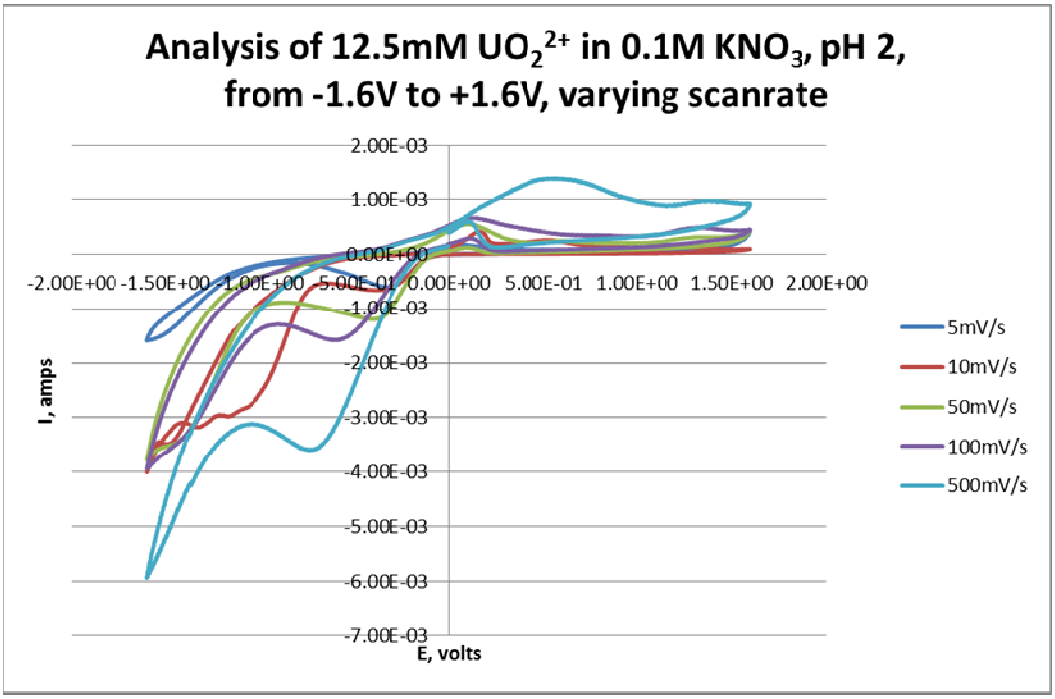

Figure 3.9A CV overlay of a 12.5 mM solution of uranyl nitrate in 0.1 M KNO3 at different scan rates. A BDDE is used as the WE.

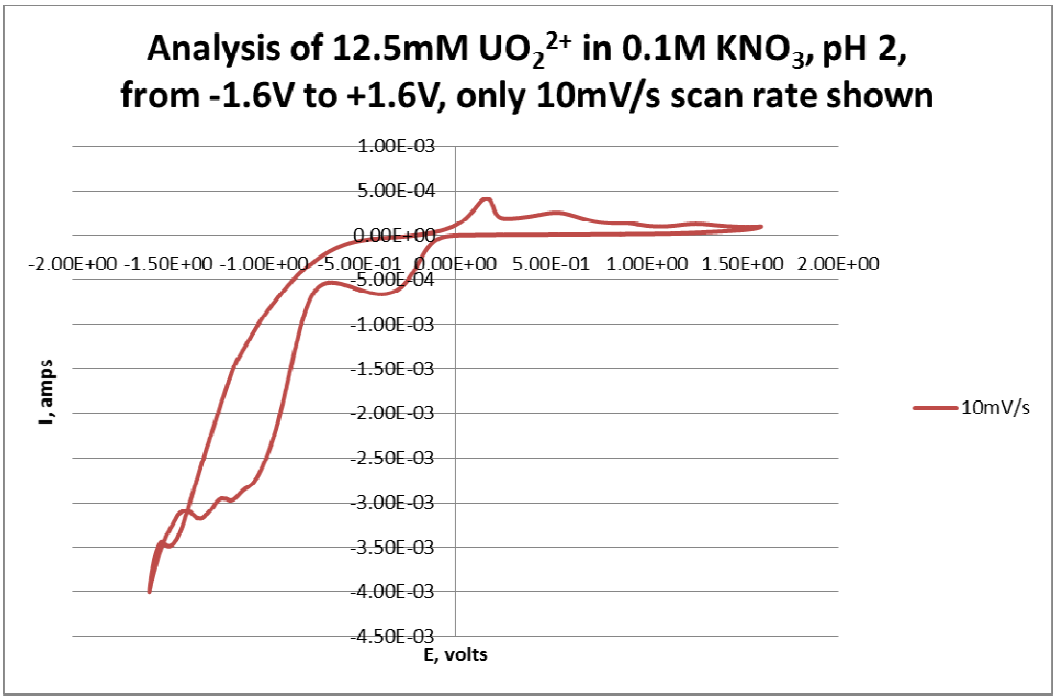

Figure 3.9B An extension of Figure 3.9A where all scan rates except for the 10mV/s are removed to allow better visibility of the electron transfer events occurring at this scan rate. A BDD WE is used.

The Figure 3.9B differs from Figure 3.9A in that the 500mV/s scan rate is removed to show the features in the slower scan rates, specifically the 10mV/s. None of the other ranges is shown in the documents since the 10mV/s scan rate best shows all of the electron transfer events in the expected reduction range. Three peaks are observed only in the 10 mV/s scan rate. The scan rates both slower and faster do not show these peaks. Instead, there is a single prominent peak, in the reduction scheme, that appears between -0.5 V and -0.9 V, which shifts more negatively as the scan rates increase, which indicates a quasi-reversible behavior. Also, there is another peak that starts at about -1.1 V and also shifts more negatively as the scan rates increase as well as a shoulder peak near the same value. There are corresponding oxidative peaks that also show up, which

shift to the more positive regions as the scan rates increase, again indicating quasi-reversible kinetics.

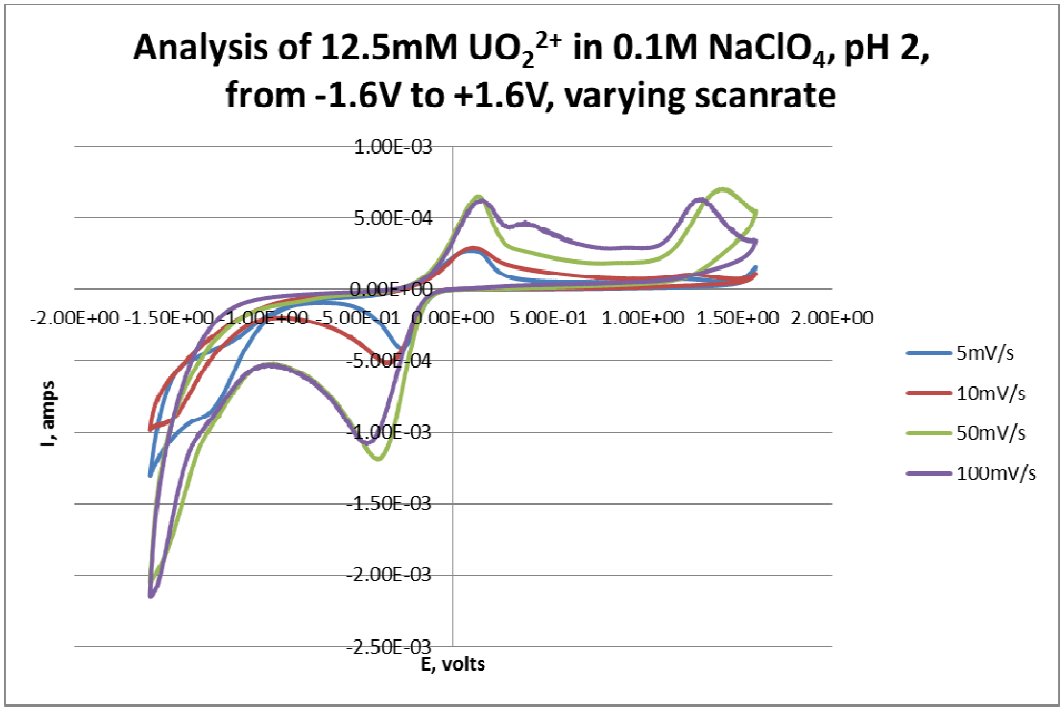

Figure 3.10 A CV overlay of a 12.5 mM solution of uranyl nitrate in 0.1 M $NaClO_4$ at different scan rates. A BDDE is used as the WE.

The same details can be seen Figures 3.10 and 3.11 with $NaClO_4$ and KCl, respectively. Both supporting electrolytes systems also demonstrate multiple reduction and oxidation peaks, which typically exhibit increasing peak potential difference (ΔE_{pp}), as scan rate increases. This indicates quasi-reversible kinetics.

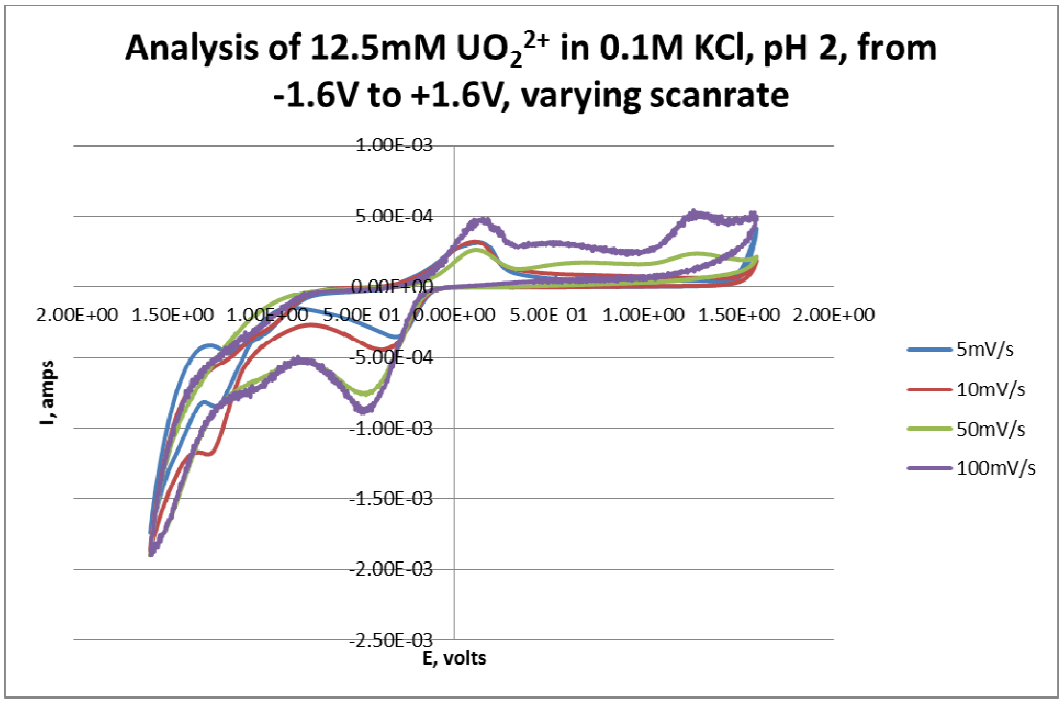

Figure 3.11 A CV overlay of a 12.5 mM solution of uranyl nitrate in 0.1 M KCl at different scan rates. A BDDE is used as the WE.

The next two Figures 3.12 and 3.13 are the same SE systems as seen in previous figures but at lower concentrations. The intensities of the peaks decreased in a manner consistent with decrease in concentration but only the most intense peaks at roughly -0.6 V and a shoulder at -0.9 V remain obvious in the cathodic region. There are still several oxidation peaks in the positive region of the CV. The hypothesis is that the third reduction peak is shifted more cathodic due to slow kinetics.

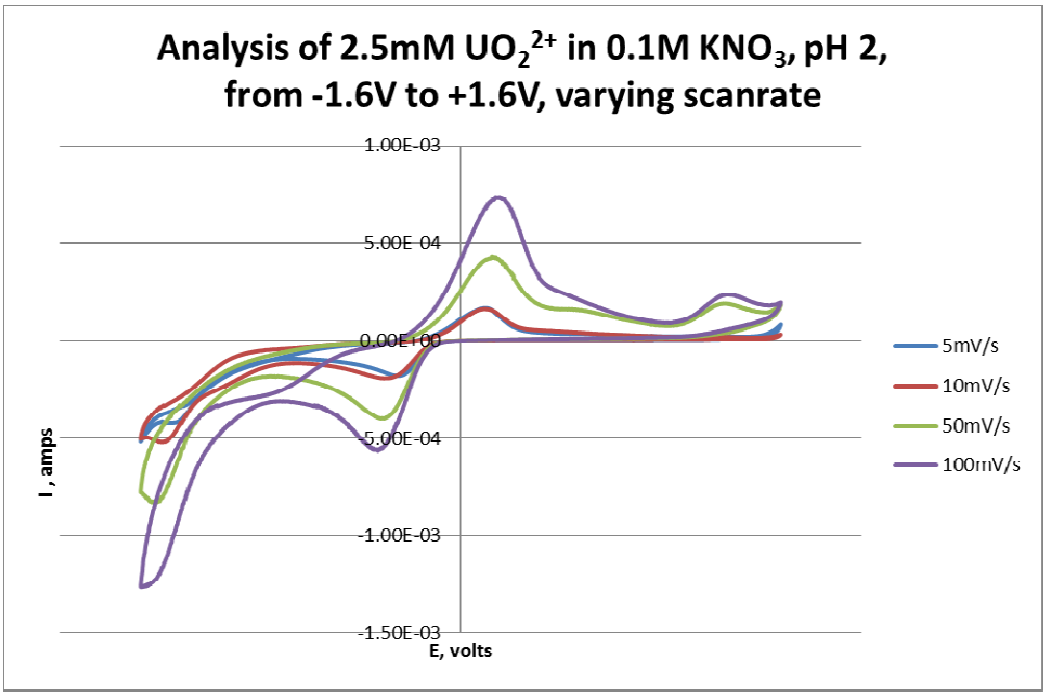

Figure 3.12 CV overlay of a 2.5 mM solution of uranyl nitrate in 0.1 M KNO_3 at different scan rates. A BDDE is used as the WE.

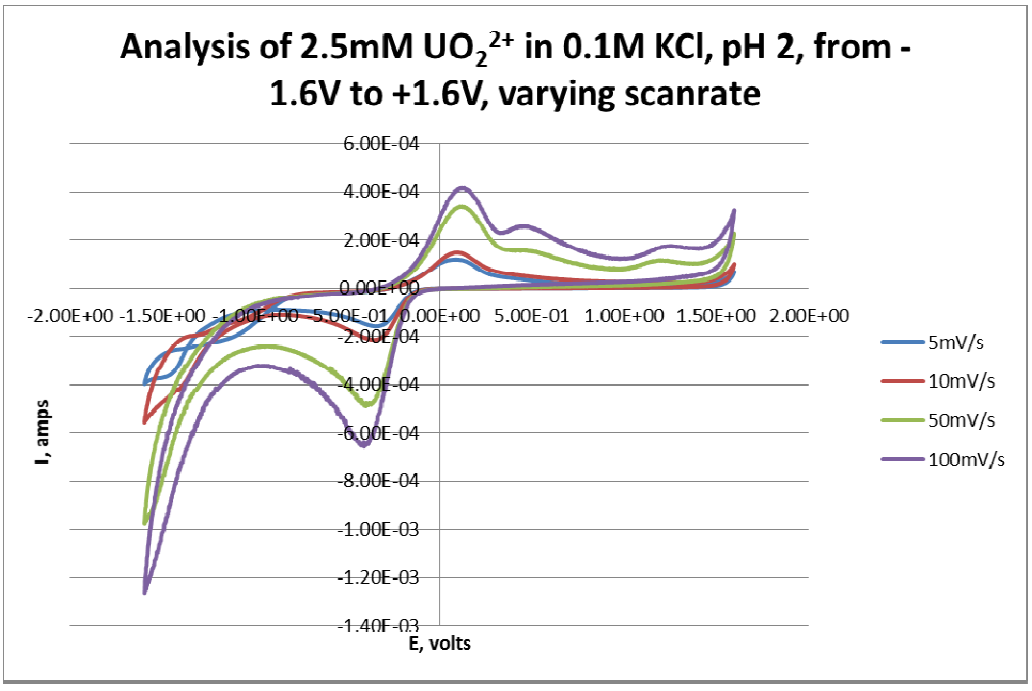

Figure 3.13 CV overlay of a 2.5 mM solution of uranyl nitrate in 0.1 M KCl at different scan rates. A BDDE is used as the WE.

The next set of experiments returned to the simplicity of the Pt working electrode. There are many advantages to the Pt electrode. It is less expensive than the BDDE, easily cleaned, and chemically inert and physically robust. The Pt WE also demonstrated greater sensitivity to the electrochemical processes in the cell. The next set of results are of UO_2^{2+} at a higher concentration, the highest concentration being 25 mM, but it is obvious that there are three reductions occurring at every scan rate with a corresponding oxidation wave or peak. The peak to peak in potential is smaller than in the BDDE systems. This suggests that the BDDE has a higher over potential and contributes to slower electron transfer kinetics. There is a peak at approximately -0.4V, -0.6V, and -0.75V, as seen in Figure 3.14, that also do not shift as dramatically as with the BDDE electrode.

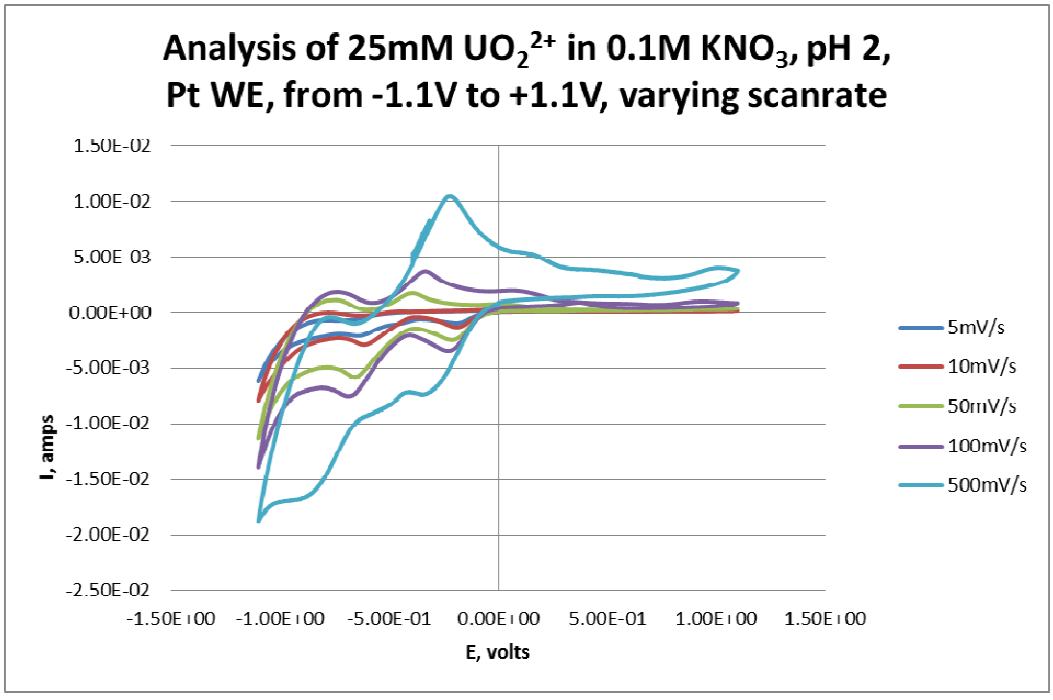

Figure 3.14 25 mM uranyl nitrate and 0.1 M KNO_3 supporting electrolyte with a Pt WE. This figure demonstrates clearly three distinct reduction and oxidation events

The same phenomenon is seen in both Figures 3.15 and 3.16. While both of these results have different characteristics specific to the SE in each, there are still obviously three reduction and oxidation peaks, which are all located between -0.25 and -1.0 V in the cathodic region and -0.75 and +0.5 V in the anodic region. Having the three reduction and oxidation peaks in all three systems demonstrates that the U(VI) to U(V), U(V) to U(IV), and U(IV) to U(III) occurs in distinct and discrete steps, and it is not a concerted process.

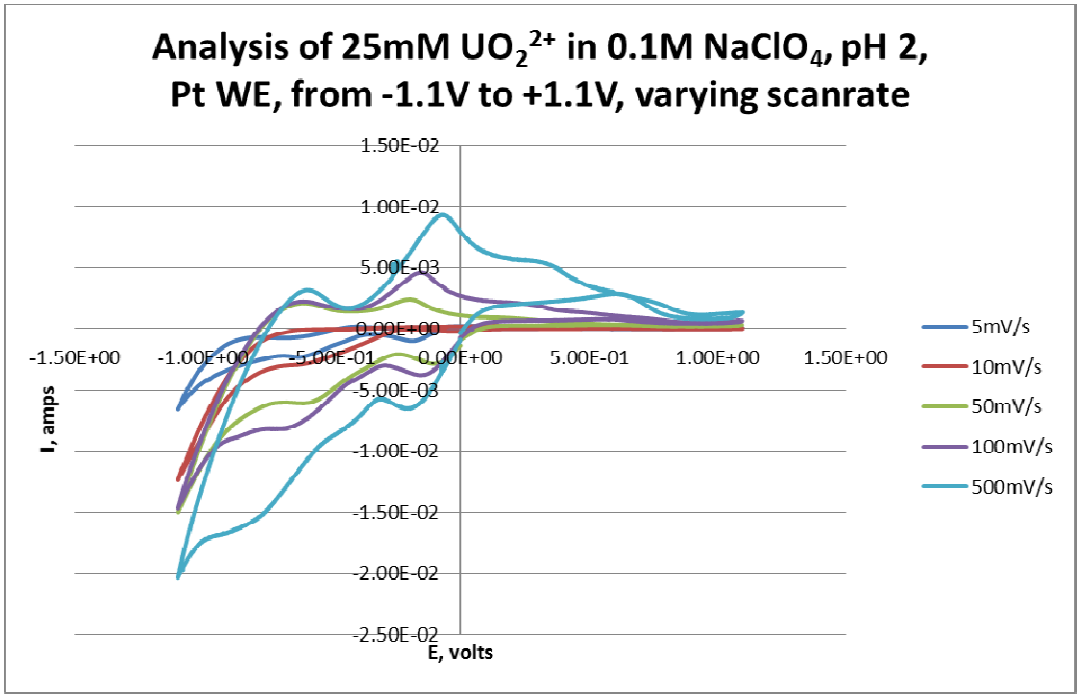

Figure 3.15 25 mM uranyl nitrate and 0.1 M $NaClO_4$ SE with a Pt WE. This figure demonstrates clearly three distinct reduction and oxidation events.

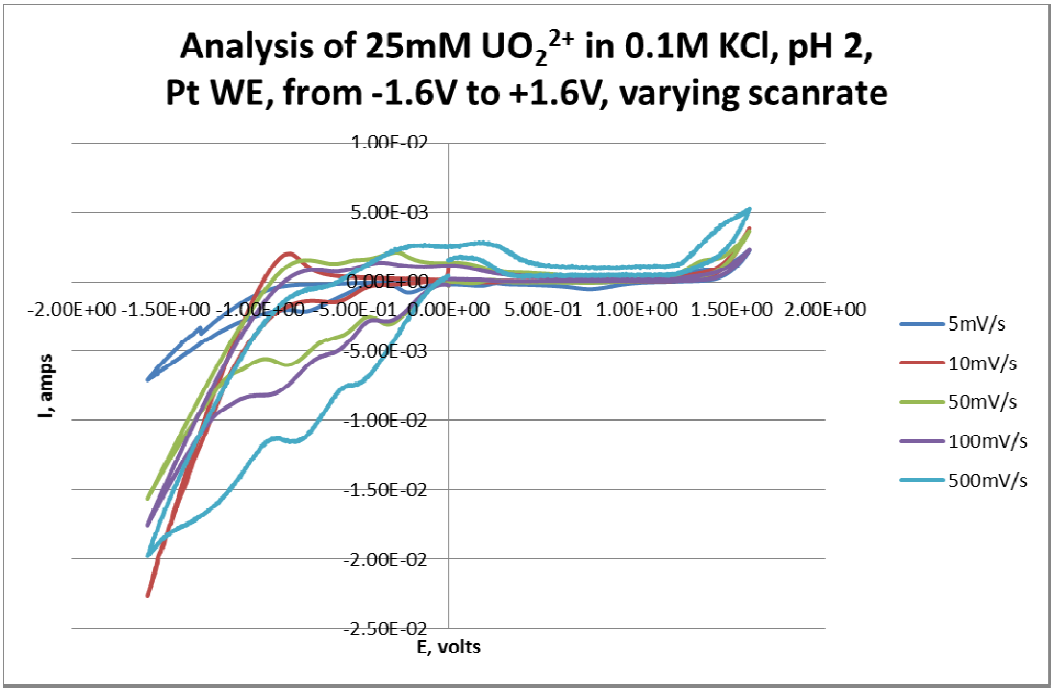

Figure 3.16 25 mM uranyl nitrate and 0.1 M KCl SE with a Pt WE. This figure demonstrates clearly three distinct reduction and oxidation events.

It definitely shows there are multiple reduction and oxidation events on both the BDDE and the Pt working electrodes and that these electron transfer events happen at different potentials. The Tables 3.1 and 3.2 give the locations of the reduction and oxidations with different working electrodes, different concentrations, and different scan rates. In Table 3.1, which shows uranium reduced on a BDD working electrode has the greatest current intensity at the 10 mV/s scan rate indicating the most electron transfer events. It is also evident that the ΔE_{pp} shifts with the reduction becoming more cathodic and the oxidation becoming more anodic as the scan rate increases. Another observation is that the current increase is proportional to the increase in concentration of uranium in solution. There are also several unknown electron transfer events, which may be associated with an intermediate species, which is also electro-active since this behavior is only observed at certain scan rates. The peaks identified are all maximum intensities and

are not base line corrected. They serve to show the same pattern of behavior in a relative manner. All cathodic and anodic activity remains consistently on the same side of the x-axis respectively.

Table 3.1 The reduction potentials for the three expected reductions in sequence at three different concentrations of uranyl in KNO_3 on the BDD working electrode. The 10mV/s scan rate shows the best results for all three reductions.

[UO22+]	SR	6-->5		5-->4		4-->3		unk		5-->6		4-->5		3-->4		unk	
		EpC1	ipC1	EpC2	ipC2	EpC3	ipC3	EpC4	ipC4	EpA1	ipA1	EpA2	ipA2	EpA3	ipA3	EpA4	ipA4
25	500	-0.548	-4.64E-03							0.152	9.82E-04	0.431	1.85E-03	1.33	3.10E-03		
	100	-0.443	-2.35E-03					-1.54	-4.71E-03	0.111	4.80E-04	0.548	4.17E-04	1.28	2.09E-03		
	50	-0.43	-1.65E-03					-1.53	-3.69E-03	0.107	4.10E-04	0.455	3.06E-04	1.24	7.76E-04	-0.597	-4.73E-05
	10	-0.378	-1.75E-03	-0.848	6.91E-04	-1.29	-2.43E-03			0.113	4.03E-04	0.426	2.22E-04			-1.22	-6.62E-04
	5	-0.331	-7.79E-04			-1.39	-1.97E-03			0.049	2.16E-04	0.411	2.29E-05	1.18	7.07E-05	-1.38	-1.23E-03
12.5	500	-0.74	-3.60E-03							0.575	1.38E-03			1.37	9.69E-04		
	100	-0.584	-1.57E-03			-1.41	-3.38E-03			0.15	6.49E-04	0.87	3.27E-04	1.32	4.82E-04	-0.653	-2.95E-05
	50	-0.395	-1.20E-03			-1.46	-3.49E-03			0.094	5.49E-04	0.585	2.42E-04	1.31	3.09E-04	-0.643	-8.76E-05
	10	-0.347	-6.53E-04	-1.17	-2.97E-03	-1.32	-3.18E-03	-1.07	-2.80E-03	0.186	3.37E-04	0.53	2.54E-04	0.887	1.34E-04	1.27	1.24E-04
	5	-0.322	1.69E-04							0.07	1.69E-04			1.15	1.73E-04		
2.5	500	-0.495	-1.08E-03							0.248	1.55E-03			1.44	4.42E-04		
	100	-0.461	-5.64E-04			-1.55	-1.25E-03			0.223	7.13E-04			1.37	2.32E-04	-0.549	-5.56E-05
	50	-0.385	-4.00E-04			-1.52	-8.29E-04			0.18	4.20E-04	0.595	1.58E-04	1.35	1.85E-04		
	10	-0.363	-1.94E-04	-1.22	-2.53E-04	-1.49	-5.22E-04			0.164	1.52E-04	0.469	4.82E-05	1.27	4.82E-05	-1.02	-6.38E-05
	5	-0.311	-1.81E-04			-1.42	-4.17E-04			0.151	1.16E-04			1.26	2.96E-05		

The data shown in Table 3.2 is for the same reduction and oxidation, but with Pt as the working electrode. Only one concentration is shown and several scan rates, which are consistent to Table 3.1. In this case, with the Pt electrode vs the BDDE, the reductions corresponding to (VI) to U(V) and U(V) to U(IV) are seen in every scan rate. Only the fastest scan rate, 500 mV/s, shows all three reductions.

Table 3.2 The reduction potentials for the three expected reductions in sequence on a Pt working electrode. 25 mM uranyl in KNO_3. The 500mV/s scan rate is the only scan rate to show all three reductions. This is significantly different than the BDDE system.

WE	SR	6-->5		5-->4		4-->3		unk		5-->6		4-->5		3-->4		unk	
		EpC1	ipC1	EpC2	ipC2	EpC3	ipC3	EpC4	ipC4	EpA1	ipA1	EpA2	ipA2	EpA3	ipA3	EpA4	ipA4
Pt	500	-0.333	-7.36E-03	-0.521	-8.26E-03	-0.876	-1.66E-02			-0.195	1.01E-02	0.155	5.20E-03	0.444	3.78E-03	-0.741	5.40E-04
	100	-0.261	-3.42E-03	-0.671	-7.51E-03					0.075	1.95E-03	-0.304	3.44E-03			-0.705	1.74E-03
	50	-0.205	-2.47E-03	-0.652	-5.82E-03					0.058	7.11E-04	-0.362	1.59E-03			-0.75	1.12E-03
	10	-0.18	-1.33E-03	-0.644	-2.88E-03					0.009	2.29E-04	-0.454	3.96E-05			-0.767	-6.27E-05
	5	-0.187	-9.78E-04	-0.638	-2.11E-03			-0.474	-1.09E-03							-0.844	-8.09E-04

There are still unidentified electron transfer events, which may be indicative of an electroactive intermediate species in this system as well.

The next set of results shown is from a concentration study. This was conducted in the PTFE minicell with a BDDE WE, a Pt wire CE, and an Ag/AgCl RE. The concentration of the uranium was varied. The SE was 0.1 M KNO_3 and the pH was set at 2.0 using HNO_3. Both Figures 3.17 and 3.18 demonstrate that as concentration of the uranium increased so did the currents of the reductive and oxidative peaks. This is consistent at different scan rate demonstrating a concentration dependence to the reduction and oxidation sequence. The data suggest that the electrochemical reduction of uranium follows a complex mechanism that is both scan rate and concentration dependent. Refer back to Tables 3.1 and 3.2, which show the reduction potentials of uranium in the experiments with both the BDDE and Pt working electrodes.

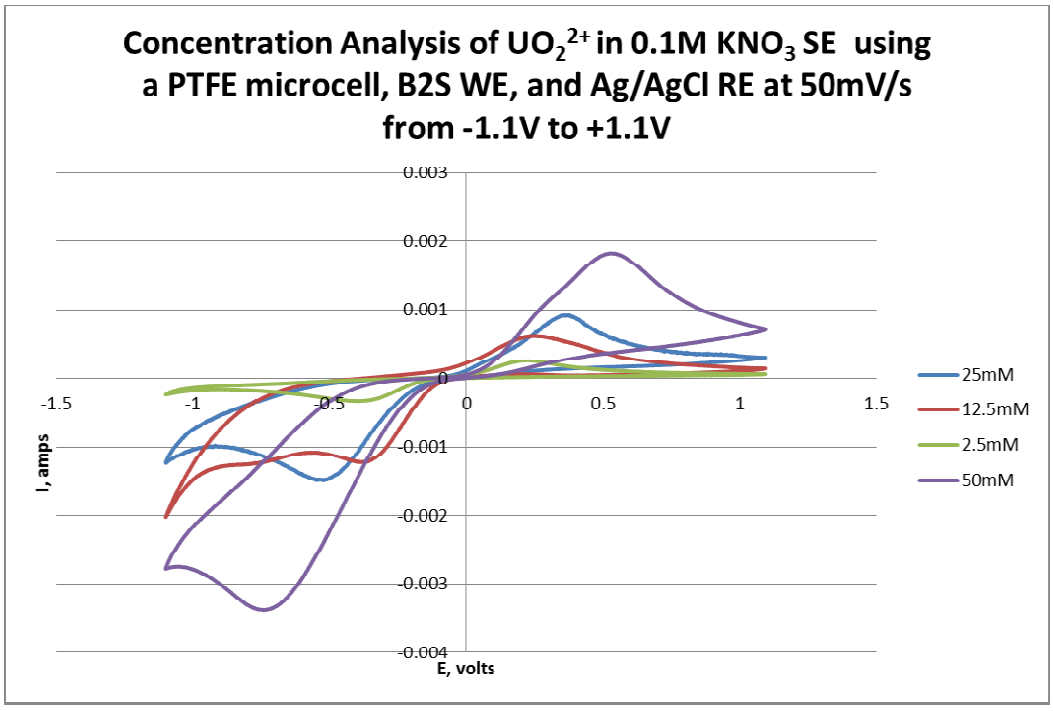

Figure 3.17 Four different concentrations of uranium with the first reduction and oxidation steps visible. This is BDDE WE system and all CV's were conducted at 50mV/s.

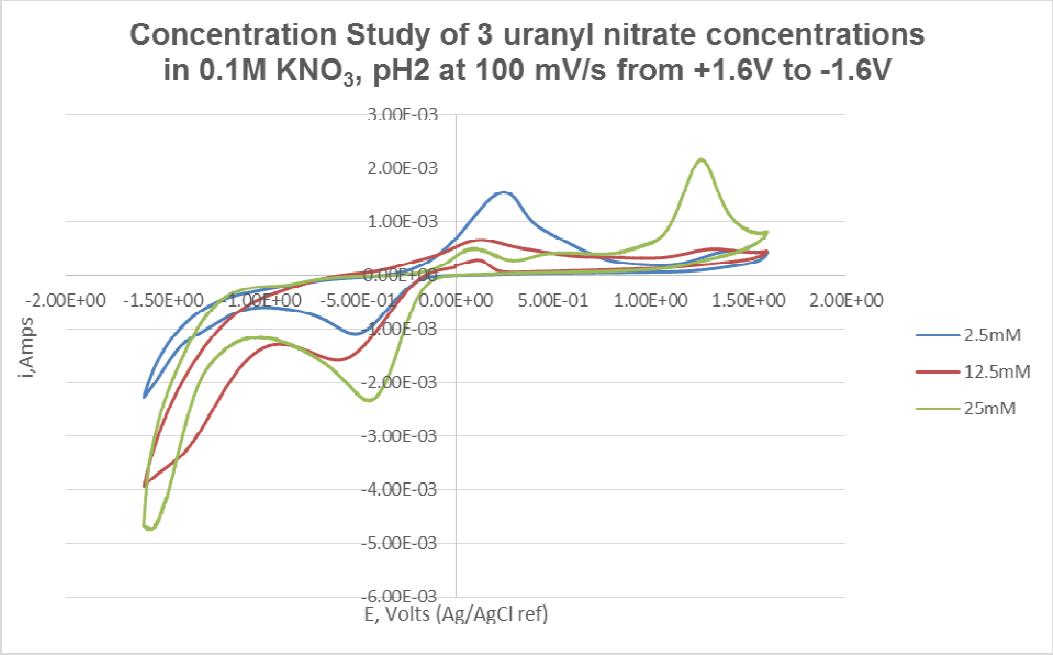

Figure 3.18 Three different concentrations of uranium with a larger reduction and oxidation range. This is BDDE WE system and all CV's were conducted at 100mV/s.

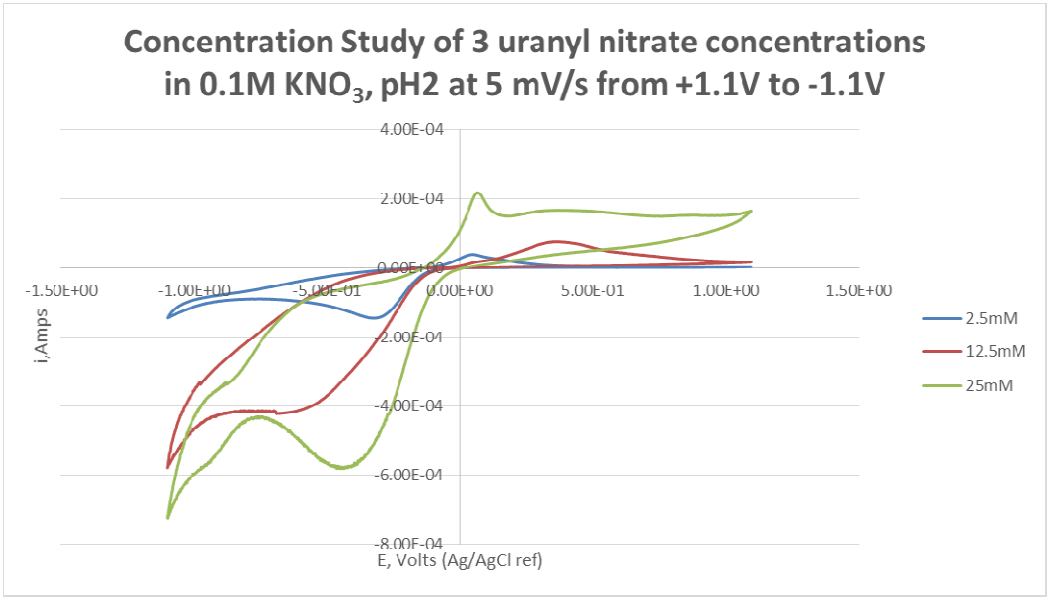

Figure 3.19 Three different concentrations of uranium with a smaller reduction and oxidation range (+1.1V to -1.1V). This is BDDE WE system and all CV's were conducted at 5 mV/s.

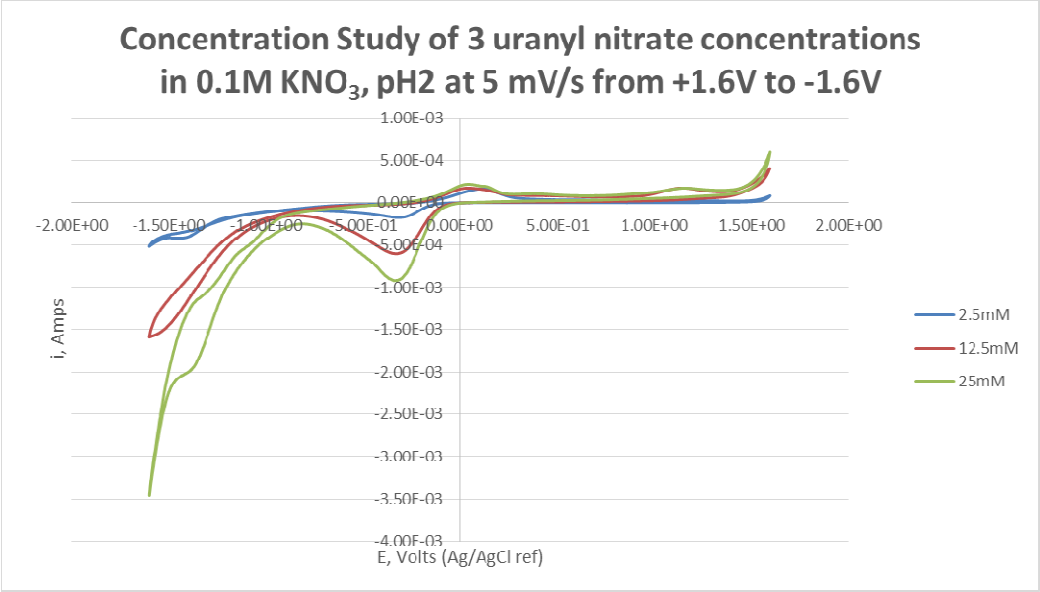

Figure 3.20 Three different concentrations of uranium with a larger reduction and oxidation range. This is BDDE WE system and all CV's were conducted at 5 mV/s.

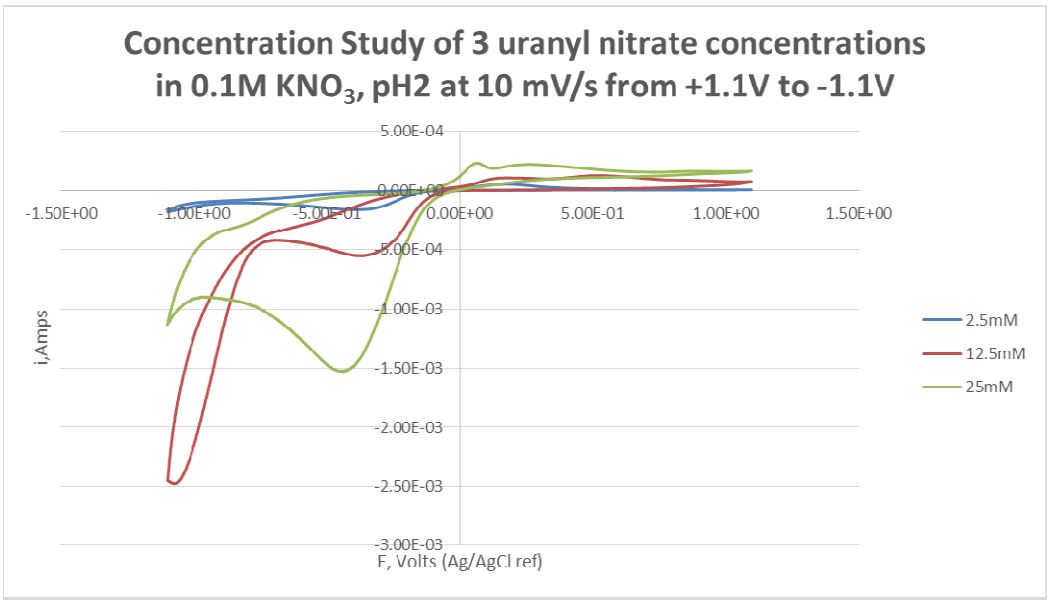

Figure 3.21 Three different concentrations of uranium with a smaller reduction and oxidation range (+1.1V to -1.1V). This is BDDE WE system and all CV's were conducted at 10mV/s.

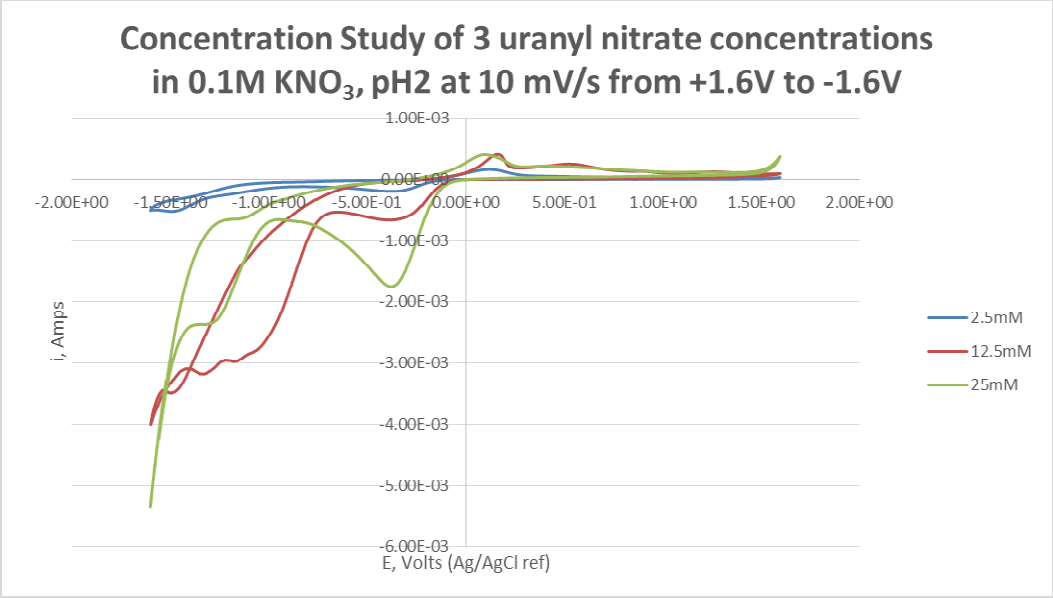

Figure 3.22 Three different concentrations of uranium with a larger reduction and oxidation range. This is BDDE WE system and all CV's were conducted at 10 mV/s.

Figures 3.17 and 3.18 show concentrations ranging from 50mM to 2.5 mM at 50 mV/s with a prominent reduction peak at -0.6V for all concentrations, and then as a contrast, at 100mV/s. What can be seen is one electron transfer event in each case. Figures 3.18 through 3.22 show a series of CV's with three concentrations of uranyl nitrate in 0.1 M KNO_3 at pH2. In both ranges, +/- 1.1V and +/-1.6V at 5mV/s a prominent reduction peak can be seen with a smaller second peak at around -1.1V. In the scan rate at 5mV/s, three electron transfer events are observed right at -1.1V.

The platinum working electrode gave more sensitive current response, therefore another series of experiments was conducted. The next experiment used only HNO_3 as the supporting electrolyte, which provides both charge carrying capacity and pH control. This system is least complex solution in terms of total ionic strength and provides clear evidence that the reduction of uranium to U(III) is attainable in any system. This

electrolyte solution does not resemble a nuclear processing stream, but should still represent support of the reduction of uranium in the least complex setup in a minicell with Pt as the working electrode. The supporting electrolyte was 0.025 M HNO_3, pH 2.0 solution was used with a 5.0 mM uranyl nitrate analyte. The voltage range was from +0.01 V to -0.90 V and scan rate was varied from 1000 mV/s to 50 mV/s in 50 mV/s increments were all conducted in an inert N_2 environment.

The result of that experiment is shown in Figure 3.23. All twenty CV's are overlaid to show the three electron transfer events. The current is a function of scan rate, which accords with theory. The potentials of the peaks shift more cathodic with an increase in scan rate indicating quasi-reversible kinetics.

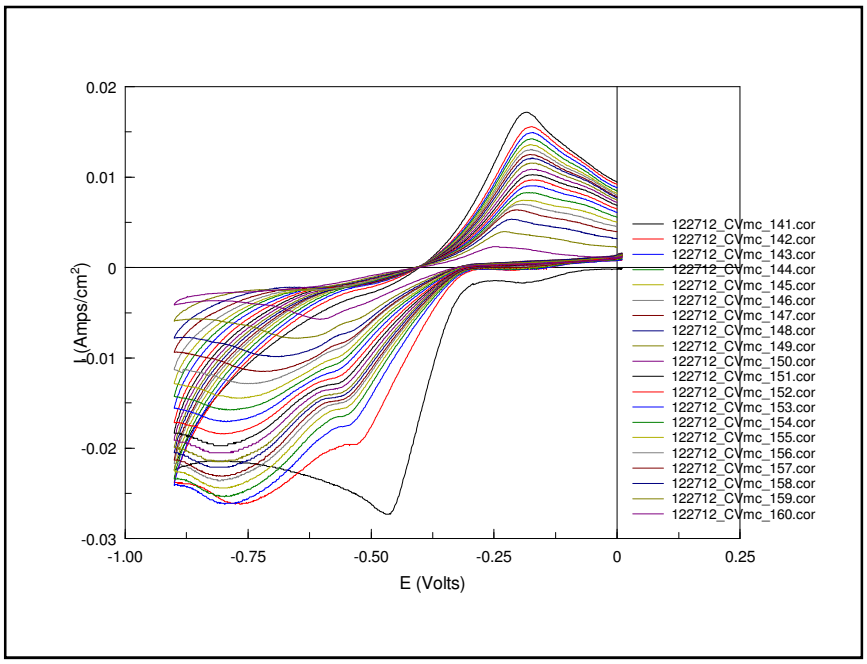

File 122712_CVmc_141 represents 1000mV/s and each additional CV represents a drop of 50mV/s per scan ending with the final scan of 50mV/s which is file 122712_CVmc_160

Figure 3.23 Twenty CV overlay of a 5.0 mM uranyl nitrate in 0.025 M HNO_3 SE. The scan rates range from 1000 mV/s to 50 mV/s in 50 mV/s increments. The three reduction events are seen as a function of the scan rate where two are prominent and the third is hard to identify as it is minute in comparison.

And as before in Figures 3.14 and Table 3.2, the fastest scan rate has the biggest, most prominent peak associated with the U(VI) to U(V) reduction. As the scan rates decrease, the first reduction event shifts and then another reduction event, U(V) to U(IV) appears, and eventually the final reduction U(IV) to U(III) can also be seen.

Another consideration to be made is whether the reduction is occurring at or near the surface of the electrode, or conversely whether it is occurring on the electrode by adsorbing. The following two figures compare the current versus scan rate (Figure 3.24A), and the current versus the square root of the scan rate (Figure 3.24B). Both of these data sets are plotted and then compared where the most linear of the two line fits determines which is true in this system. In the system, using a BDD working electrode, the more linear line fit was the in Figure 3.24B. This indicates that the reductions occur near the

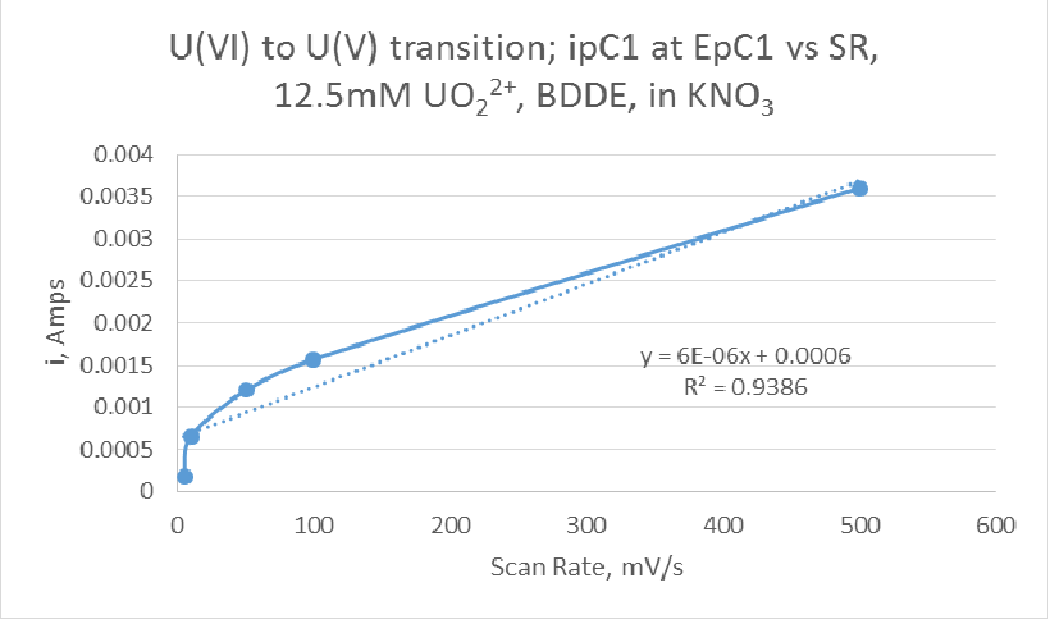

Figure 3.24A The current plotted as a function of scan rate. This is the 12.5 mMuranyl nitrate in the minicell with the BDDE. The R^2 value is 0.9386.

the surface of the electrode and not on it, per electrochemical theory. The R^2 value of the line with the square root of the scan rate is 0.9911, whereas the plot of current as a function of scan rate had an a R^2 of 0.9386.

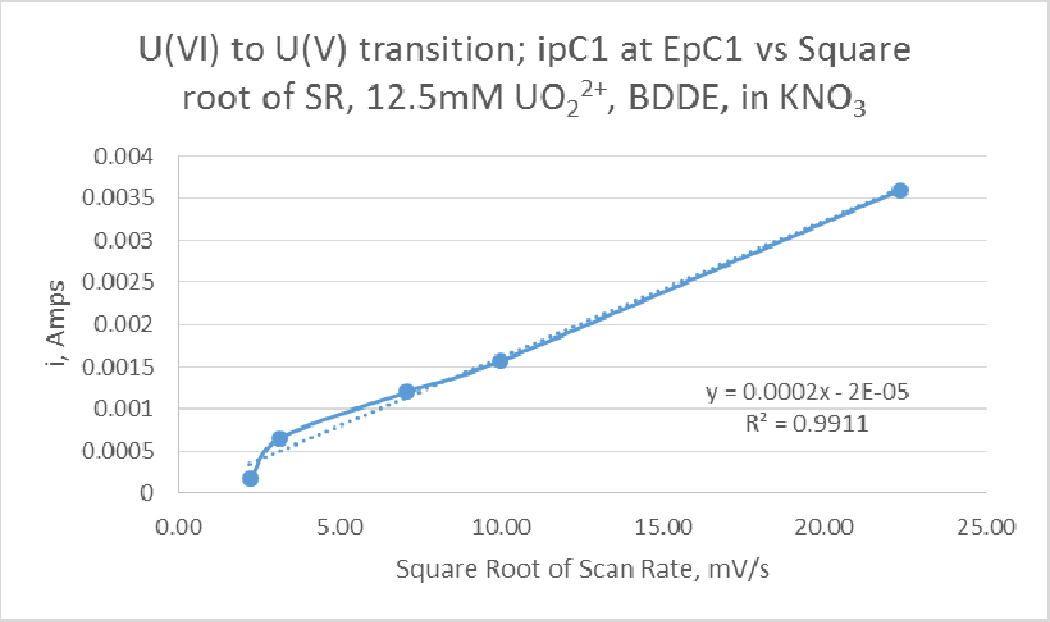

Figure 3.24B Cyclic voltammetric current plotted as a function of the square root of the scan rate. 12.5 mM uranyl nitrate in the minicell with the BDDE. The R^2 value is 0.9911.

The next figures show the same reduction of U(VI) to U(V) but on the Pt working electrode instead. All other experimental parameters are the same. Again the more linear line fit in the two figures is in Figure 3.25B, where the current is plotted as a function of the square root of the scan rate.

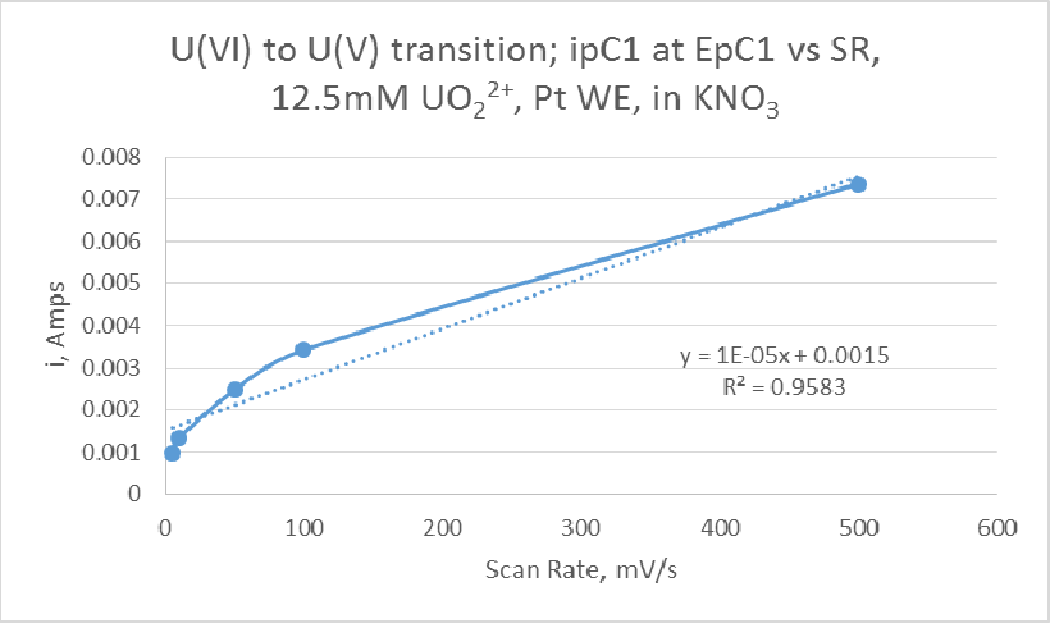

Figure 3.25A. Cyclic voltammetric current plotted as a function of scan rate. 12.5 mM uranyl nitrate in the minicell with the Pt. The R^2 value is 0.9583.

The two R^2 values are quite different, demonstrating quite clearly that this a solution-based reduction happening near the electrode surface and definitely not on it.

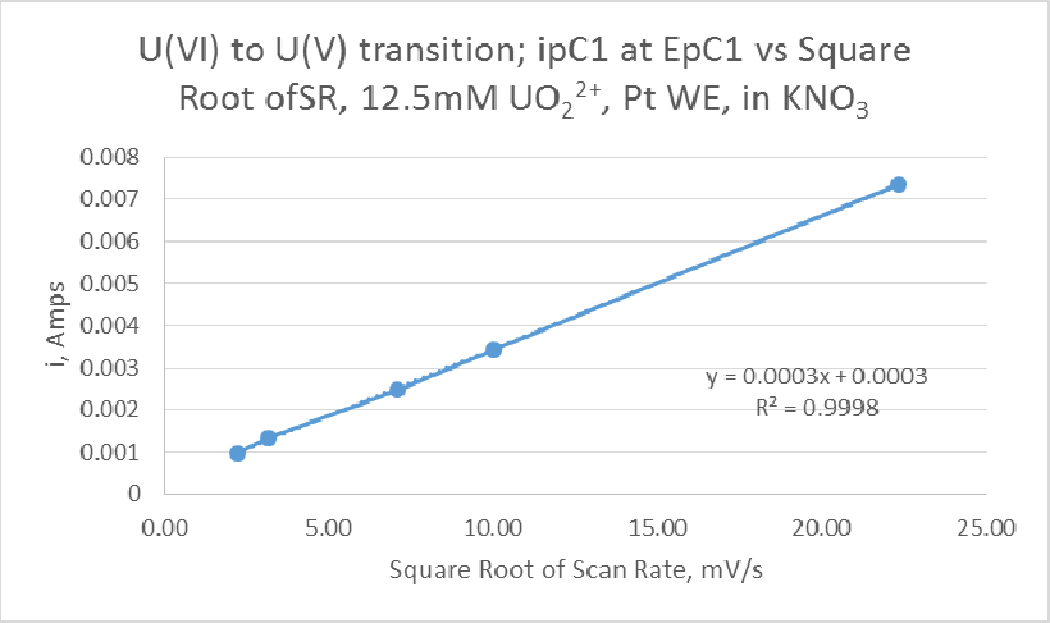

Figure 3.25B Cyclic voltammetric peak current plotted as a function of the square root of the scan rate. T 12.5 mM uranyl nitrate in the minicell with the Pt working electrode. The R^2 value is 0.9998.

Spectroscopic Analysis of Uranium Reduction

Electrochemical reduction of uranium is evident based on CVs but secondary confirmation was pursued. One standard method of verifying a species existence is to show its presence spectroscopically. UV-Vis is used to identify the metal species directly and Raman spectroscopy is used to verify indirectly by measuring the evolution and extinction of specific uranium-oxygen bonds. Using the specialized SEC, which allows simultaneous electrochemical manipulation and spectroscopic analysis, several different experiments were conducted to verify either directly or indirectly that all oxidation states of uranium had been achieved as expected.

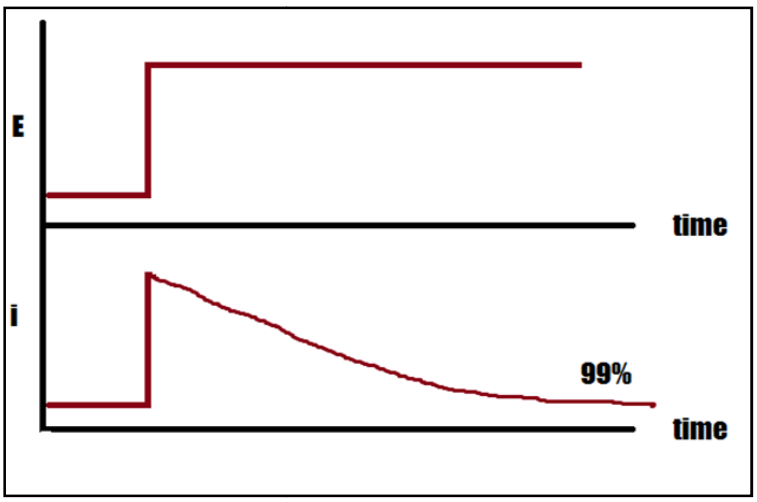

With CPE:

1. If i decays as $t^{-1/2}$, then possible to determine the number of electrons transferred
2. $\int i dt = nFE^{o}$

Figure 3.26 The generic format for the controlled potential electrolysis which is used for all of the SEC experiments. A potential is set and the resulting current decay is measured.

The cyclic voltammetric experiment is too fast at most scan rates for the spectroscopic techniques to measure the products. A controlled potential electrolysis technique was used to maintain the reduction potental across the solution/electrode interface of the WE during spectroscopic measurement of the electrochemical products. Figure 3.27 shows the base line spectra of three different SE's containing 25.0 mM U(VI). There was no potential applied so that only the U(VI) and the supporting electrolyte would be observed.

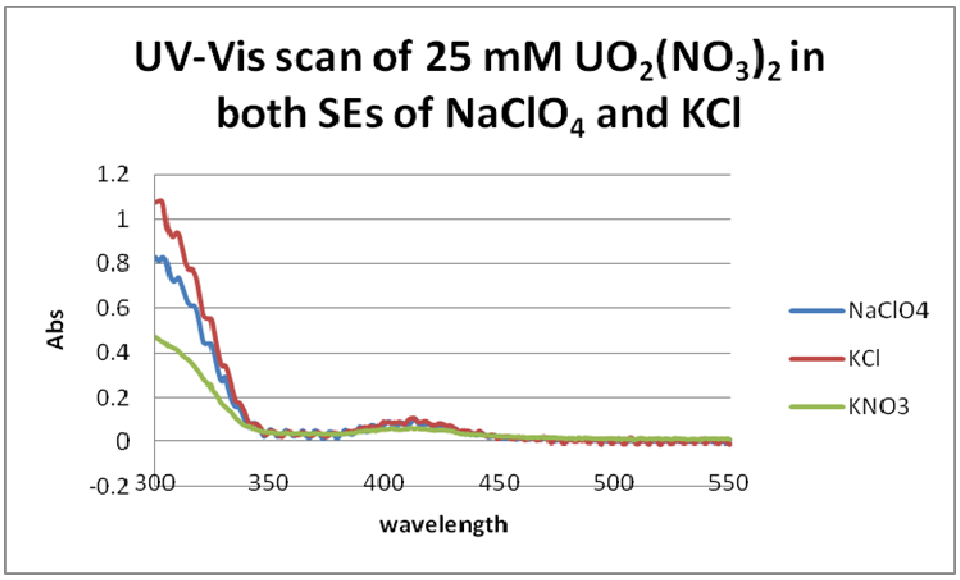

Figure 3.27 Overlay of UV-Vis spectra of two different supporting electrolyte solutions containing 25.0 mM UO2(NO3)$_2$ in the UV-Vis SEC. Applied potential is zero. The small broad peak at 420 nm is associated with U(VI).

In Figure 3.28, a solution of 0.1 M KNO_3 containing 10mM uranyl nitrate is placed in the special UV-Vis SEC. A potential of -2.1V was applied for 3 minutes while the UV-Vis scanned from 500 to 300 nm. There was N_2 flowing over the cell and the pH was at 2.9. The UV-Vis spectrum shows three distinct peaks, which correspond to the three oxidation states of uranium expected. This spectrum is consistent with literature values.[24][25] The yellow KNO_3 baseline shown was recorded separately with no uranyl nitrate present.

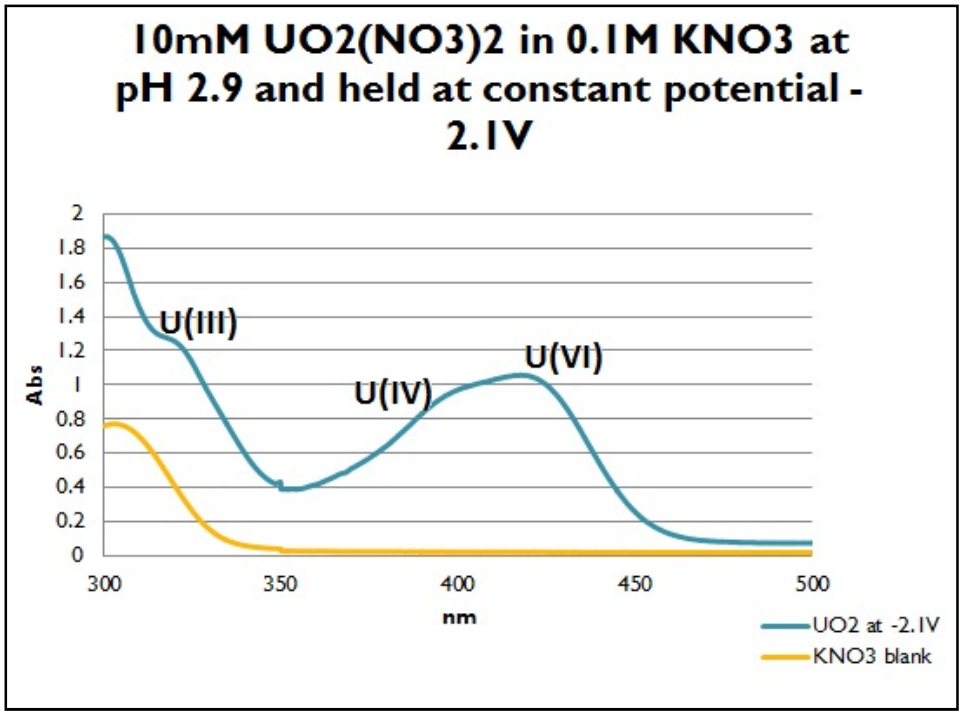

Figure 3.28 UV-Vis SEC results showing defined peaks of U(III), U(IV), and U(VI).

Another specialized cell used was the Raman SEC, which was to be used an indirect method to show the reduction of uranyl. This was accomplished by observing the extinction of the uranium – oxygen double bond, which is the uranyl – axial oxygen double bonds and the evolution of the single bond, which is the uranium – oxygen bond associated with U(VI). Additionally, it would be able to diagnose uranium – ligand interactions intended for solvent extraction separations, which will be future work in this project.

In Figure 3.29, several WE surfaces are compared via Raman analysis. They are boron doped diamond, glassy carbon, and vapor deposited diamond. The spectrum in the middle is the BDDE used in this project. The region highlighted by the green box is

where peaks associated with uranium-oxygen bonds, as well as nitrates, are to be expected.

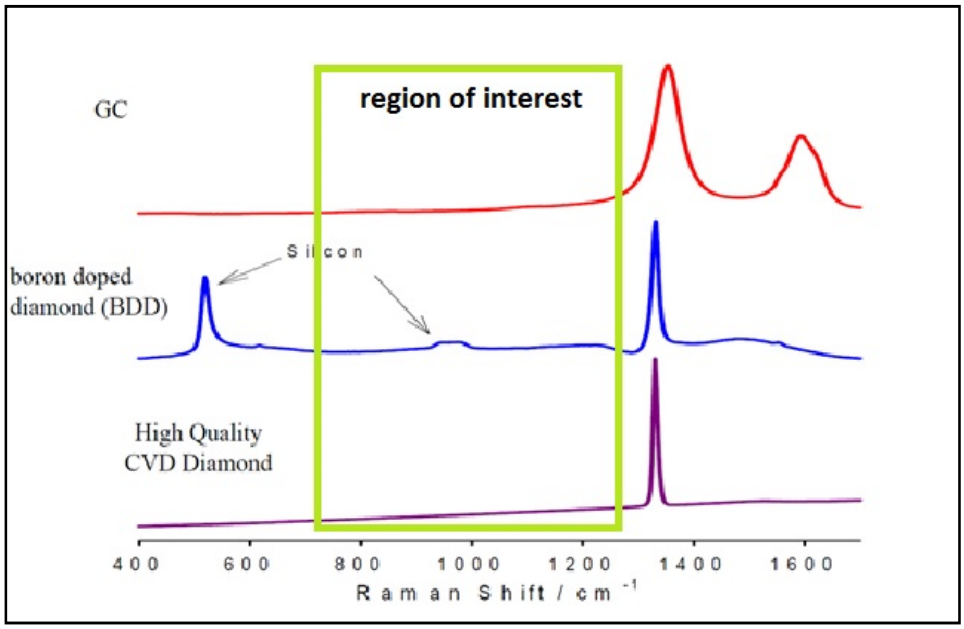

Figure 3.29 Raman spectra of planar electrode surfaces. The blue curve is the BDD surface used in this work, in the Raman SEC. The green blocked region is where Raman peaks should appear for the solutions and analytes. The BDD surface exhibits no interferences in the region of interest.

Figure 3.30 shows several spectral overlays. The blue spectrum is a 25mM solution of uranyl nitrate in 0.1 M KNO_3. The working volume of this cell is roughly 0.5 mL and the solution is purged with N_2 prior to injecting it into the cell, which is then capped and sealed. The nitrate and uranyl peaks are prominent in prior to the controlled potential electrolysis experiment. When the potential is applied at -2.1 V, another Raman spectrum is taken, shown in yellow. The reduced uranyl peak is smaller, leading to its identification as U(V) and the nitrate peak remains constant. Neither U(IV) or U(III) can be detected directly with Raman techniques as they no longer are Raman active species as they are no longer symmetric molecules. It is important to note that

U(III) is a vigorous chemical reducing agent, and it reduces the materials of the cells. After conducting this experiment, the cells were so damaged they had to be remade.

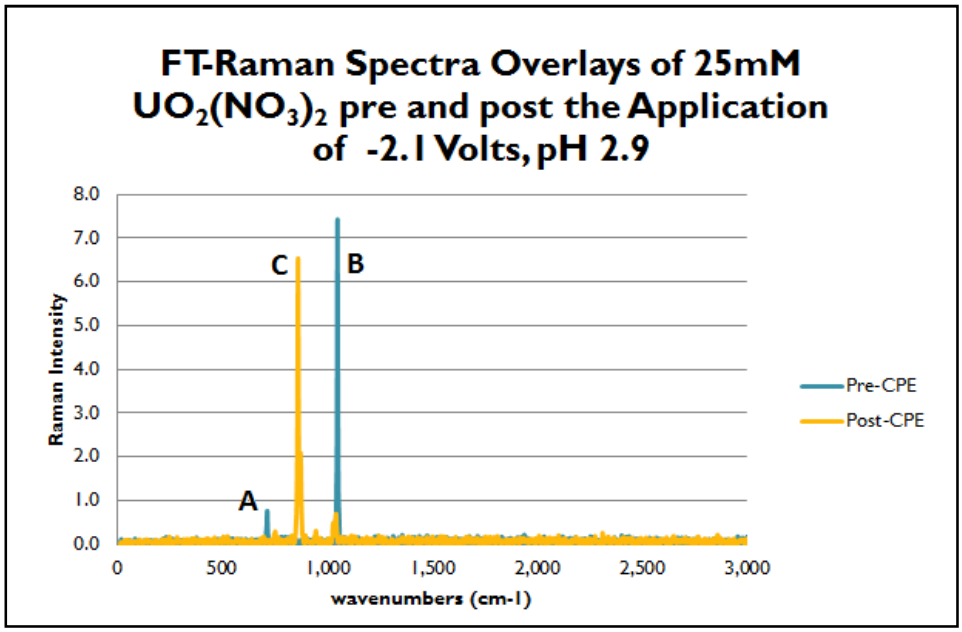

Figure 3.30 Overlay of two Raman spectra. A 25mM $UO_2(NO_3)_2$ solution was used in the Raman SEC. The blue curve is the solution before a constant potential of -1.6V is applied. The yellow spectrum is the uranium solution while a constant potential of -1.6 is applied. Peak A is -NO_3, peak B is U=O, and peak C is the reduced uranium species

This results demonstrate that uranium can easily be reduced to U(III) and kept in that oxidation state long enough in the SEC's to record spectra, which takes approximately one to three minutes. The electrochemical reduction is predicable, can be done in various supporting electrolyte solutions, and at different pH's. The reduction does not appear concentration dependent but is scan-rate dependent.

CHAPTER FOUR: CONCLUSIONS AND DISCUSSION

Original Project Goals

Originally, this project was only a small piece of a much larger project involving the simple task of reducing uranium(VI) to U(III) to compare its coordination sphere characteristics to other actinides. As the project progressed, it became apparent that creating U(III) in aqueous solution was no trivial issue. As a result, several important questions became the focus of this project. These questions are:

1. Can Uranium be reduced to U(III) in aqueous conditions?
2. Can Uranium be reduced to U(III) in strongly acidic aqueous condition similar to a nuclear waste stream?
3. What are the optimal conditions for the reduction of U(VI) to U(III) in acidic aqueous medium?
4. Is U(III) stable for a period of time long enough to perform spectroscopic analysis and possible chemical coordination?

It has been clearly shown that uranium can be reduced to each oxidation state in an aqueous environment, in the presence of various electrolytes such as KNO_3, $NaNO_3$, $KClO_4$, $NaClO_4$, NaCl, KCl, and in HNO_3, in various types of cells, such as a standard glass cell, minicell, and specialized spectroelectrochemical cells (SEC's), and on either Pt or boron doped diamond working electrode. The reduction to multiple oxidations states

of uranium was possible in various pH's, however lower pH's demonstrated less energy was required to add each successive electron. This reduction is corroborated by spectroscopic findings showing multiple oxidation states in solution during the controlled potentiometric electrolysis.

In this work, we have thoroughly characterized the electrochemistry of uranium in aqueous environments similar to those expected in nuclear power plant waste streams. The simplest supporting electrolyte system, 0.025 M HNO_3, worked well but this system is less complex than what may actually occur in the complex waste stream. The other electrolytes tested were KNO_3, $NaNO_3$, $KClO_4$, $NaClO_4$, NaCl, and KCl. The pH plays a major role in the reaction mechanism and any possible side, or unintended, reactions as well as the reduction of uranium. The acid increases the ionic strength of the solution significantly at lower pH and promotes the generation of H_2 at the cathode. However, the data shown in Figure 3.5 predicts that it should be easier to reduce all species of uranium at lower pH's. This is was found to be true.

The boron doped diamond (BDD) electrode is a semiconductor that allows a broad accessible potential range, 8 volts (+4 to -4 V) even in aqueous solutions, and is chemically inert. It can however foul over time and is brittle. Pt is also relatively inert both chemically and physically. A serious drawback to the Pt electrode is the narrow useful range in water, +1.8 to -1.0 V. The cathodic range is limited because Pt is catalytic for the reduction of hydrogen.

The third question, "What are the optimal conditions?" may not be as significant as it originally seemed. Uranium could be reduced to U(III) using either the BDD or Pt working electrodes, and in every supporting electrolyte. Pt allowed for the reduction to

U(III) between 0 to -1 V whereas with the BDD electrode there is a higher overpotential and a greater applied potential was required. Reduction to U(III) could be achieved at about -1.6V on the BDDE. The supporting electrolytes, which seemed to give the least amount of solution-based electron transfer events, were KCl and KNO_3 at low pH's. It is key to note that the targeted waste stream composition includes KNO_3 and HNO_3 at very high concentrations, therefore this solution also closely resembles the conditions for application of these findings.

Development of Specialized Electrochemical CELLS

In response to the need to develop specialized cells in order to quickly manipulate the solution and analyze the results, several new cell types were needed. In the case of the simple electrochemical cell (the "minicell"), a surface corrosion analysis cell was repurposed with minor modifications. This cell allowed for small volume to be quickly manipulated while maintaining the highest level of control over all of the experimental conditions. This minicell carried the largest workload and allowed for the analysis of all of the supporting electrolytes, electrode surfaces, pH's, and analyte concentrations with the smallest amount of time between trials and least concern for outside interferences and contaminations.

In addition to the minicell, several other specialized cells had to be fabricated to make spectroscopic analysis of the electrochemically reduced environment could be conducted. A UV-Vis cell modelled after a BASi cell was made and used to analyze the controlled potential electrolysis (CPE) reduction of uranium to U(III). Several FT-IR and FT-Raman SEC's were made as well with data taken from the FT-Raman SEC analysis shown in this work. Both of these SEC's performed as expected and resulted in

spectroscopic evidence of the reduction of uranium and also for future use in the specific ligation and extraction of the actinides.

Elucidation of the Electrochemistry of Reduction of U^{6+}

This work has resulted in a proposed mechanism for the step-wise reduction of U(VI) to U(III). The multiple CV's show through scan rate analysis that the reductions all occur by quasi-reversible kinetics. This is proven by ΔE_{pp} changing with scan rates and by the increasingly cathodic potential at which each electron transfer event occurs as a function of increasing scan rate. Concomitantly, the corresponding oxidative steps all shift more anodic for each electron transfer. The scan rate dependence can be used to determine the heterogeneous rate constants. Future work should explore this but the 10mV/s scan rate on the BDD working electrode gave the clearest set of reduction peaks, suggesting that both faster and slower scan rates are not optimal. This was demonstrated by looking at the 5mV/s, 10mV/s, and 50mV/s scan rates. The only scan rate that showed all three electron transfer events was the 10mV/s scan rate with the BDDE, as seen in Figures 3.9 through 3.13. In these systems, at fast scan rates, the scan is over before the quantitative electron transfer can from U(V) to U(IV) to occur as electrode kinetics can't keep up. However, going too slowly may allow an irreversible homogeneous step to occur. Based on the electrochemical results, an EC'EC'E mechanism is proposed, where each "E" stands for electrochemical step and "C'" stands for a chemical step with an intermediate conformation or competitive reaction.

(1) E $UO_2^{2+} + e^- \rightarrow UO_2^+$ **U(VI) to U(V)**, see Note 1

(2) C' Outer sphere reorganization

Disproportionation of U(V) to U(IV) and U(VI), (Concentration dependence) See Note 2

(3) E $4H^+ + UO_2^+ + e^- \rightarrow U^{4+} + 2H_2O$ **U(V) to U(IV)**, see Note 3

(4) C' Inner and outer sphere reorganization and competitive reaction as U(IV) is adsorbed to cathode (removed from solution)vs U(IV) → U(III), see Note 4

(5) E $U^{4+} + e^- \rightarrow U^{3+}$ **U(IV) to U(III)**, see Note 5

Note 1: Step (1) is reversible, fast, least reorganization

Note 2: The disproportionation follows the mechanism:

$2UO_2^+ + 4H^+ \leftrightarrow UO_2^{2+} + U^{4+} + 2H_2O$ U(V) ↔ U(VI) and U(IV)

Note 3: Step (2) is quasi-reversible,

Note 4: The competitive reaction is between the $U(IV)_{aq} \rightarrow U(III)_{aq}$ and

$n\,(U(IV)_{aq} + U(IV)_{aq}) \rightarrow nU(IV)_s$

Note 5: Step (3) is quasi-reversible, fast

There are differences in the CV's when the Pt versus the boron doped diamond working electrode is used but the overall mechanism of the sequence of reductions is the same. When Pt is used for the working electrode, unlike with BDDE, all three electron transfer events can be seen through a range of scan rates. See Figures 3.14 through 3.16. This difference between the two electrodes needs to be explained. Pt is a conductor and there is little to no resistance to the flow of electrons, so electron transfer steps in the

mechanism can occur very quickly. The BDDE on the other hand is a semi-conductor that has an inherently higher resistance to electron flow within the material than the Pt. This means that the scan rate required to capture an electron transfer event will be slower with the BDD than a Pt working electrode. This is a benefit as it allows for the ability to isolate single reductions and determine the rate constants and kinetics of each step.

The first step of the mechanism is very fast and is consistent regardless of concentration or scan rate. Step (2) must be two, sequential or competitive, slow reactions. An outer sphere rearrangement where the electron is transferred from the solvent into the uranium molecule and a slow disproportionation of highly unstable U(V) to U(VI) and to U(IV), both of which are more stable. If the scan rate is fast enough to produce U(V), then U(IV) can also be produced in the next reduction before the U(V) ions diffuse from the double layer back into the bulk solution and revert to U(VI). If the scan rate is too slow, then there will be an interruption in the reduction process and neither U(V) nor (IV) will be evident. There will always be some of each oxidation state made as the appropriate potential is achieved just due to the diffusion of ions to the cathode, but they may not be detectable. This is why only one large peak can be seen at higher scan rate versus multiple smaller peaks at lower scan rates. The amount of disproportionation products formed is a function of the scan rate in the CV. The higher the scan rate, the more U(V) is formed to the point that the formation of U(VI) ions cannot be detected at the cathode and shows little to no current.

Step (3), the reduction of U(V) to U^{4+} is another fast electron transfer. If there is U(V) present at the cathode, then as the potential is applied to reduce the ion it will readily and completely reduce.

Step (4) is the second "C'" step and there is another outer sphere rearrangement where another electron is transferred from the solution directly to the uranium molecule, which then requires inner sphere rearrangement as the uranium oxygen bonds are broken. Additionally, there is a competitive reaction taking place where U(IV) can either accept another electron to produce U(III), which is thermodynamically unstable, or bond with other U(IV) ions to form the mineral urananite and adsorb to the cathode. Evidence suggesting the adsorption is twofold. First, there is a larger shift cathodically as the reduction potential to uranium(III) is greater. This is interpreted as the deposition of a layer of the insulator uranite being formed. And second, visual inspection of the electrode surface shows a yellowish residue, which is difficult to remove. The final mechanism step is also proposed to be a fast step. It produces the unstable U(III) species and is dependent on the formation of U(IV). There is a competing process in which the formation of U(IV) adsorbs to the surface of the electrode and is removed from the solution, which results in small U(III) peaks in the cyclic voltammetry.

Uranium reduction is apparent from the cyclic voltammetry data but to support this hypothesis it was important to have a corroborating method. The method of choice is spectroscopy, and both UV-Vis, to determine the metal ion present in solution, and FT-IR and FT-Raman to analyze bonds within the molecule were employed. These will also be the methods used in future work to explore the ligand– metal interactions.[23][25][51-60] The U(V) species was not observed in the spectra even though the electrochemical evidence shows there was at least some U(V) produced. It seems that the U(V) species was not long lived enough or produced in quantities sufficient to be observed by the UV-Vis. This is consistent with a fast disproportionation step, as proposed in the mechanism. The

spectroelectrochemical experiment was performed by imposing a constant voltage of -2.1 V vs. SRE, which was maintained for 3 minutes as the UV-Vis spectrum was recorded from 500 nm to 300 nm at a scan rate of just over 1 nm/s. In Figure 3.28, a uranyl solution was scanned and peaks at 320 nm, 400 nm, and 440 nm were detected, which were consistent with the literature values for U(III), U(IV), and U(VI), respectively.[23][25][53][55][56]

The Raman spectroelectrochemical system provided indirect evidence to support identification of the peak associated with the uranium-oxygen double bond at 1100 cm^{-1}. The FT-Raman SEC provided both direct and indirect evidence to support the electrochcemical reduction of uranium. The spectra taken prior to the applied potential showed a prominent peak associated with the U(VI) uranyl, linear double bond and a smaller nitrate peak. When the potential was applied to the cell, there was a prominent peak shift from 1000 cm^{-1} to 800 cm^{-1}, which is proposed here to be U(V) slightly angled double bonds. There is still evidence of the presence of U(VI) in the solution but at a much lower level at the surface of the electrode where the Raman is focused. It is not possible to detect the U(IV) or U(III) species with the Raman, but it is assumed that these oxidation states are also present in solution, near the electrode surface as the potential applied is sufficient to reduce uranium to these species.[63][64][65]

It should be remembered that the purpose of this study was to put uranium in an oxidation state that would permit its inclusion in a larger study of ligand extraction of the actinides from nuclear process wastes. Uranium is expected to favor greater ionic character in its coordination sphere, and the trend from uranium to the right, across the actinide series would then be toward increasing covalent character in coordination.

Being able to demonstrate this trend would be a major step toward development of a closed nuclear fuel cycle, because better ligands with stronger coordination constants could then be identified to remove the minor actinides from the waste stream. In order to find a ligand that will preferentially bind to actinides in the presence of lanthanides, it is first important to level the playing field by compare the two together when their surface charge densities are identical, as then it will be possible to test what ligand binds better to MA's. In the end, the research will lend to the larger picture of finding a way to make a closed nuclear fuel cycle by finding an efficient way to extract, purify, and reuse the MA's that come of a nuclear waste stream. The work in this project will show that the electrochemical process could be used to elucidate the coordinate covalent bonding of actinides and lanthanides with the eventual goal of removing MA from a nuclear power process streams. This could then potentially reduce the amount of dangerous radiotoxic waste.

In summary, this project was originally thought to be a simple electrochemical experiment but has proven far more complex. It has been shown that uranium(VI) can indeed be electrochemically reduced to U(III), which will permit including uranium in the sequence of elements intended for ligand extraction studies. Including uranium in that larger research effort is expected to result in definitive steps toward a closed nuclear fuel cycle. On the other hand, this work has also raised several very interesting questions. The electrochemical reduction mechanism of the uranyl ion is a complex three-electron process complicated by intervening homogeneous chemical steps. Future work will seek to identify kinetic and thermodynamic parameters of that mechanism, and to support the

proposed steps in the mechanism by proving the existence of the various species involved.

Future Work

1. The kinetics of each electron transfer step can be determined by conducting very detailed scan rate studies with smaller scan rate steps.

2. The diffusion coefficients of uranyl and the other uranium species can be determined by using a rotated electrode system. Knowing the value of the diffusion coefficient permits more detailed characterization of the kinetics involved.

3. The spectroeletrochemical work with the Raman SEC will be continued by creating U(V) in the system and stopping the potential sweep, which will allow U(VI) to re-form. This rate will allow for the determination of the disproportionation kinetics. The experiment would be repeated but with U(IV) potential to watch the formation of U(V) and U(VI) simultaneously.

4. Ligands previously identified to be selective for the actinides will be used in a study of the covalency of the coordination sphere of uranium.

REFERENCES

1. U.S. Department of Energy Environmental Management - Department of Energy Five Year Plan FY 2008-FY 2012 Volume II. Released 8 April **2008**.

2. Public Health and Environmental Radiation Protection Standards for Yucca Mountain, Nevada; Proposed Rule. Environmental Protection Agency. 6 June **2008**.

3. Per P.; Kastenberg W.; Corradini M. Nuclear Waste and the Distant Future. *Issues in Science and Technology*, National Academy of Sciences, July **2006**.

4. International Atomic Energy Agency Issues relating to safety standards on the geological disposal of radioactive waste. International Atomic Energy Agency. 6 June **2008**.

5. International Atomic Energy Agency, Spent Fuel and High Level Waste: Chemical Durability and Performance under Simulated Repository Conditions, October **2007**.

6. Nuclear Regulatory Commission: Fact Sheet on Dry Cask Storage of Spent Nuclear Fuel. NRC. May 7, **2009**.

7. Vandenbosch, Robert, and Vandenbosch Susan E, Nuclear waste stalemate. Salt Lake City: University of Utah Press, 10. **2007**.

8. Yates, Marshall. DOE waste management criticized: On-site storage urged. Public Utilities Fortnightly, 6 July **1998**, 124, 33.

9. Hoare, J.P. Electrochemistry of Oxygen. Interscience Publishers, **1968**.

10. Hafemeister, David W. Physics of societal issues: calculations on national security, environment, and energy. Berlin: Springer, 187-189, **2007**.

11. Dumping and Loss overview and Subductive Waste Disposal Methods. Oceans in the Nuclear Age, March 23, **2011**.

12. Tricia Jack, Jordan Robertson, Utah Nuclear Waste Summary, Center for Public Policy & Administration, University of Utah, **2008**.

13. Rao, K.R. Radioactive waste: The problem and its management, Current science,

25 Dec **2001**, vol. 81, no. 12.

14. National Policy Analysis #396: The Separations Technology and Transmutation Systems (STATS) Report: Implications for Nuclear Power Growth and Energy Sufficiency, Feb **2002**.

15. http://www.gnep.energy.gov/pdfs/GNEP_SOP

16. Freidberg, JP., Department of Nuclear Engineering: Reports to the President 2000-2001. MIT Review, Aug **2012**.

17. About the Blue Ribbon Commission on America's Nuclear Future. December **2012**, http://cybercemetery.unt.edu/archive/brc/20120620211605/http:/brc.gov//.

18. Blue Ribbon Commission on America's Nuclear Future. Disposal Subcommittee Report to the Full Commission. December **2012**.

19. Apostalakis G., Hejzlar P., Shwageraus, E., The future of the nuclear fuel cycle; an MIT interdisciplinary study, CANES press, **2011**.

20. Management of Spent Fuel at Nuclear Power Plants. IAEA Bulletin. January **2008**.

21. The Preparation of the EFTTRA-T5 Americium Transmutation Experiment. Seventh Information Exchange Meeting on Actinide and Fission Product Partitioning and Transmutation. October **2002**.

22. Herrman S.D.; Li S.X. Separation and recovery of uranium metal from spent light water reactor fuel via electrolytic reduction and electrorefining. *Nuclear Technology*, **2010**, Vol. 171, 247-265.

23. Cotton S.A. Scandium, yttrium, the lanthanides, and the actinides; *Annu. Rep, Prog, Chem. Sect. A*, **2005**, Vol 101, 294-318.

24. Katz J.J; Seaborg G.T; and Morss L.R. The Chemistry of the Actinide Elements, Vol 1, 2 Ed., Chapman and Hall LTD, London, **1986**, 169 – 442.

25. Cotton S.A.; Lanthanide and Actinide Chemistry, John Wiley and Sons LTD, **2006**.

26. Herrman S.D.; Li S.X. Separation and recovery of uranium metal from spent light water reactor fuel via electrolytic reduction and electrorefining. *Nuclear Technology*, **2010**, Vol. 171, 247-265.

27. Kocherov, N; Lammer M.; Schwerer, O. Handbook of Nuclear Data for Safeguards, International Atomic Energy Agency, INDC(NDS)-376, December **1997**.

28. Loveland, W. D.; Morrissey D.J.; Seaborg, G.T.; Modern Nuclear Chemistry, Wiley, **2006**.

29. Nash, K.L.; Lumetta, G.J. Ed. Advanced Separation Techniques for Nuclear Fuel Reprocessing and Radioactive Waste Treatment, Woodhead, **2011**.

30. Kihara, S.; Yoshida, Z.; Aoyagi, H.; Maeda, K.; Shirai O.; Kitatsuji, Y.; Yoshida Y. A Critical Evaluation of the Redox Properties of Uranium, Neptunium and Plutonium Ions in Acidic Aqueous Solutions," Pure Appl. Chem. **1999**, 71(9), 1771-1807.

31. Bockris J.O'M., Reddy A.K.N.; Modern Electrochemistry 1, Ionics, 2nd Ed., Kluwer Academic Publishers, **2002**.

32. Bockris J. O'M, Reddy A.K.N.; Modern Electrochemistry 2A, Fundamentals of Electrodics, 2nd Ed., Kluwer Academic Publishers, **2002**.

33. Bockris J. O'M., Reddy A.K.N.; Modern Electrochemistry 2B, Electrodics in Chemistry, Engineering, Biology, and Environmental Science, Kluwer Academic Publishers, **2002**.

34. Bard A.J, Faulkner L.R.; Electrochemical Methods; Fundamentals and Applications; John Wiley and Sons Inc., **2001**.

35. Saito,E.; Souza, F.A; Azevedo, A.F.; Ferreira, N.G.; Baldan, M.R. Electrochemical Determination of the Real Area of Nanocrystalline Boron Doped Diamond. *ECS Trans*. **2012**, 43(1): 169-176.

36. Martin, H.B.; Argoitia, A.; Landau, U.; Anderson, A.B.; Angus, J.C. Hydrogen and Oxygen Evolution on Boron-Doped Diamond Electrodes. *J. Electrochem. Soc*. **1996**, 143(6), 133-136.

37. Carlos, S.; Oliveira, B.; Oliveira-Brett, A. Voltammetric and electrochemical impedance spectroscopy characterization of cathodic and anodic pre-treated boron doped diamond electrode. *ElectrochimicaActa*, **2010**, Vol. 55, 4599-4605.

38. Kissinger P.T., Heiniman W.R.; Laboratory Techniques in Electroanalytical Chemistry; Marcel Dekker, New York, **1996**.

39. White D. A.; Fathurrachman, A. An experimental investigation of uranium redox reaction in an electrolytic cell with a cation exchange membrane. *Journal of Radioanalytical and Nuclear Chemistry*, **1997** Vol. 218. No. 1, 27-33.

40. Kissinger, P.T.; Heiniman, W.R. Laboratory Techniques in Electroanalytical Chemistry; Marcel Dekker, New York, **1996**.

41. Goeting, C. H.; Marken, F.; Gutierrez-Sona, A.; Compton, R.G.; Foord, J. S. Boron-

doped diamond electrodes: growth, surface characterization and sono-electrochemical applications. *New Diamond and Frontier Carbon Technology*, **1999**, Vol. 9, No. 3, 207-228.

42. Grenthe, I.; Fuger, J.; Koning, R. J. M.; Lemire, R. J.; Muller, A. B.; Nguyen-Trung C. Warner H.. Chemical Thermodynamics of Uranium. OECD NEA report, Elsevier, **2004**.

43. Morris D. Redox energies and kinetics of uranyl coordination complexes in aqueous Solution. *Inorganic Chemistry*, **2002**, Vol.41, No. 13, 3542-3547.

44. Makhfouk, M.; Meray, M.; Castebon, A.; Astruc, M. Effect of citrate, oxalate, and pyrophosphate ligands on the electrochemical reduction of the uranyl ion in a perchloric acid medium. *Bulletin of Electrochemistry*, **2002**, Vol. 18, No. 2, 63-71.

45. Wei, Y.Z.; Fang, B.; Arai, T.; Kumagai, M. Electrochemical reduction of uranium(VI) in nitric acid-hydrazine solution on glassy carbon electrode. *Journal of radioanalytical and nuclear chemistry*, **2004**, 262 (2), 409-415.

46. Asakura, T.; Astruc, M. Study on reduction of neptunium and uranium in nitric acid solution using flow type electrolytic cell, as a basic technique for advanced reprocessing process. *Journal of nuclear science and technology*, **2002**, suppl. 3, 340.

47. Koltunov, V. The kinetics and mechanism of the reduction of neptunium (VI) ions by uranium (IV) ions in nitric acid. *Radiochimicaacta*, **2002**, 90 (5), 259-267.

48. Trubachev, A.V.; Shumilova M.A.; Trubecheva L.V. Voltammetric behavior of uranium(VI) in sulfuric acid solutions containing pyridine. *Journal of analytical chemistry*, **2002**, 57 (3), 235-242.

49. Pippin C.; Sullivan J.; Meisel D.; Chopin, G. Kinetics of uranium(VI) reduction in aqueous polyelectrolyte systems. *Radiochimica Acta*, **1992**, 57 (4), 177-190.

50. Yoon, P.; Harada, Y.; Hiroshi, M.T.; Ikeda Y. Photochemical reactions of uranium(VI) in aqueous phosphoric acid solutions. Reactions with halogen and pseudohalogen anions. *Journal of Nuclear Science and Technology*. **1991**, 28(5), 418-425.

51. Orecchio, S.; Piazzese, D.; Romano, V.; Zingales, R. The formal redox potential of the U(IV-III) couple at 25^{o}C in the aqueous 3 M (Na+, H+) Cl- medium. *Annali di Chimica*. **1998**, Vol. 88, No. 1-2, 129-137.

52. Zelic, M.; Lovric, M. Isopotential points in square-wave voltammetry of reversible electrode reactions. *Collect. Czech. Cjem. Commun*. **2009**, Vol. 74, No. 10, 1489-1501.

53. Mauerhofer, E.; Zhernosekov, K.; Rosch, F. Limiting Transport Properties and hydration numbers of actinyl ions in pure water. *Radiochimica Acta*, **2004**, Vol. 92, issue 1, 5-10.

54. Suzuki, Y.; Nankawa, T.; Francis, A.J.; Ohnuki, T. Redox behavior or Ce(IV)/Ce(III) in the presence of nitrilotriacetic acid: a surrogate study for An(IV)/An(III) redox behavior. *Radiochim. Acta*, **2010**, Vol. 98, 397-402.

55. Awakura, Y.; Sato, K.; Majima, H.; Hirono, S. The measurement of the diffusion coefficient of U(VI) in aqueous uranyl sulfate solutions. *Metallurgical transactions B, Process metallurgy*, **1987**, Vol. 18, No. 1, 19-23.

56. Mizuguchi, K.; Park, Y.; Tomiyasu, H. Electrochemical and spectroelectrochemical studies on uranylcarbonato and aqua complexes. *Journal of Nuclear Science and Technology*, **1993**, Vol. 30, No. 6, 542-548.

57. Quiles, F.; Nguyen-Trung, C.; Carteret, C.; Humbert, B. Hydrolysis of Uranyl(VI) in acidic and basic aqueous solutions using a noncomplexing organic base: A multivariate spectroscopic and statistical study. *J. Inorg. Chem*., **2011**, Vol. 50, 2811-2823.

58. Quiles, F.; Burneau, A. Infrared and raman spectra of uranyl(VI) oxo-hydroxo complexes in acid aqueous solutions: a chemometric study. *Vibrational Spectroscopy*, **2000**, Vol. 23, No. 1, 231-241.

59. Toth, L.M.; Begun, G.M. Raman spectra of uranyl ion and its hydrolysis products in aqueous HNO_3. *J. Phys. Chem*., **1981**, Vol 85, No. 5, 547-549.

60. Tian, Z.; Ren, B. Adsoption and reaction at electrochemical interfaces as probed by surface enhanced raman spectroscopy. *Annu. Rev. Phys. Chem*., **2004**, Vol 55, 197-229.

61. Peterman, D. R.; Martin, L. R.; Klaehn, J. R.; Harrup, M. K.; Greenhalgh, M. R.; Luther, T. A. Selective separation of minor actinides and lanthanides using aromatic dithiophosphinic and phosphinic acid derivatives. *Journal of Radioanalytical and Nuclear Chemistry*, **2009**, 282(2), 527-531.

62. Klaehn, J.R.; Peterman, D. R.; Harrup, M. K.; Tillotson, R. D.; Luther, T. A.; Law, J. D.; Daniels, L. M. Synthesis of symmetric dithiophosphinic acids for "minor actinide" Extraction. *Inorganica Chimica Acta*, **2008**, 361(8), 2522-2532.

63. Dai, Sheng; Lee, Yuan-Hsiang; Young, J. P. Observation of the surface-enhanced Raman scattering spectrum of uranyl ion. *Applied Spectroscopy*, **1996**, 50(4), 536-537.

64. Khulbe, P. K.; Agarwal, Anshu; Raghuvanshi, G. S.; Bist, H. D.; Hashimoto, H.;

Kitagawa, T.; Little, T. S.; Durig, J. R. Raman studies of the vibrational dynamics and phase transitions in uranyl nitrate hexahydrate. *Journal of Raman Spectroscopy*, **1989**, 20(5), 283-90.

65. Duval, P. B.; Burns, C. J.; Buschmann, W. E.; Clark, D. L.; Morris, D. E.; Scott, B. L. Reaction of the Uranyl(VI) Ion (UO_2^{2+}) with a Triamidoamine Ligand: Preparation and Structural Characterization of a Mixed-Valent Uranium(V/VI) Oxo-Imido Dimer. *Inorganic Chemistry*, **2001**, 40(22), 5491-5496.